

---

The following resources related to this article are available online at <http://stke.sciencemag.org>.  
This information is current as of 29 December 2011.

---

- Article Tools** Visit the online version of this article to access the personalization and article tools:  
<http://stke.sciencemag.org/cgi/content/full/sigtrans;4/198/rs12>
- Supplemental Materials** "Supplementary Materials"  
<http://stke.sciencemag.org/cgi/content/full/sigtrans;4/198/rs12/DC1>
- Related Content** The editors suggest related resources on *Science's* sites:  
<http://stke.sciencemag.org/cgi/content/abstract/sigtrans;4/179/eg5>  
<http://stke.sciencemag.org/cgi/content/abstract/sigtrans;4/179/rs5>  
<http://stke.sciencemag.org/cgi/content/abstract/sigtrans;4/179/rs6>  
<http://stke.sciencemag.org/cgi/content/abstract/sci;332/6037/1557>  
<http://stke.sciencemag.org/cgi/content/abstract/sigtrans;3/104/ra3>
- References** This article cites 73 articles, 31 of which can be accessed for free:  
<http://stke.sciencemag.org/cgi/content/full/sigtrans;4/198/rs12#otherarticles>
- Glossary** Look up definitions for abbreviations and terms found in this article:  
<http://stke.sciencemag.org/glossary/>
- Permissions** Obtain information about reproducing this article:  
<http://www.sciencemag.org/about/permissions.dtl>

# Systematic Phosphorylation Analysis of Human Mitotic Protein Complexes

Björn Hegemann,<sup>1\*†</sup> James R. A. Hutchins,<sup>1\*‡</sup> Otto Hudecz,<sup>1,2</sup> Maria Novatchkova,<sup>1,2</sup> Jonathan Rameseder,<sup>3</sup> Martina M. Sykora,<sup>1</sup> Sihan Liu,<sup>3§</sup> Michael Mazanek,<sup>1,2</sup> Péter Lénárt,<sup>1,4</sup> Jean-Karim Hériché,<sup>4</sup> Ina Poser,<sup>5</sup> Norbert Kraut,<sup>6</sup> Anthony A. Hyman,<sup>5</sup> Michael B. Yaffe,<sup>3,7</sup> Karl Mechtler,<sup>1,2</sup> Jan-Michael Peters<sup>1||</sup>

Progression through mitosis depends on a large number of protein complexes that regulate the major structural and physiological changes necessary for faithful chromosome segregation. Most, if not all, of the mitotic processes are regulated by a set of mitotic protein kinases that control protein activity by phosphorylation. Although many mitotic phosphorylation events have been identified in proteome-scale mass spectrometry studies, information on how these phosphorylation sites are distributed within mitotic protein complexes and which kinases generate these phosphorylation sites is largely lacking. We used systematic protein-affinity purification combined with mass spectrometry to identify 1818 phosphorylation sites in more than 100 mitotic protein complexes. In many complexes, the phosphorylation sites were concentrated on a few subunits, suggesting that these subunits serve as “switchboards” to relay the kinase-regulatory signals within the complexes. Consequent bioinformatic analyses identified potential kinase-substrate relationships for most of these sites. In a subsequent in-depth analysis of key mitotic regulatory complexes with the Aurora kinase B (AURKB) inhibitor Hesperadin and a new Polo-like kinase (PLK1) inhibitor, BI 4834, we determined the kinase dependency for 172 phosphorylation sites on 41 proteins. Combination of the results of the cellular studies with Scansite motif prediction enabled us to identify 14 sites on six proteins as direct candidate substrates of AURKB or PLK1.

## INTRODUCTION

In eukaryotes, chromosome segregation depends on major structural and physiological changes in the dividing cell. These include centrosome maturation, chromosome condensation, assembly of a bipolar spindle, and bi-orientation of all chromosomes on the spindle through the formation of microtubule-kinetochore attachments. Sister chromatids are only separated from each other once all of these events have been completed, and cytokinesis is only initiated once the sister chromatids are approaching the opposite spindle poles. Errors in any of these processes or their temporal order can lead to chromosome missegregation, an event that is thought to contribute to the evolution of malignant tumor cells and, when it occurs in human oocytes, is the cause of Down syndrome (trisomy 21), a common human congenital disorder.

The molecular events that lead to chromosome segregation are mediated by numerous proteins. Most of these do not function in isolation but as multiprotein complexes, sometimes called “molecular machines” (1, 2). The properties of these machines are to a large part determined by the inherent properties of their subunits. For example, the ability of microtubules to assemble into bipolar spindles is primarily due to the physicochemical properties of their  $\alpha$ - and  $\beta$ -tubulin subunits (3). However, the precise control of the chromosome segregation “machinery” in space and time depends on numerous regulatory proteins. Most of these are enzymes that do not mediate chromosome segregation per se, but regulate these events indirectly by controlling the activities and locations of protein complexes with direct roles in chromosome segregation. Well-known regulators of chromosome segregation are cyclin-dependent kinase 1 (CDK1) (4), the Aurora kinases A and B (AURKA and AURKB), Polo-like kinase 1 (PLK1) (5), and the ubiquitin ligase anaphase-promoting complex/cyclosome (APC/C) (6). Activation of CDK1 leads to mitotic entry with concomitant activation of AURKA, AURKB, and PLK1 and, together, these kinases initiate the numerous events required for chromosome segregation. For example, CDK1 and AURKB are thought to confer rigidity to mitotic chromosomes by promoting the binding of condensin complexes to DNA, PLK1 and AURKB mediate the partial separation of sister chromatids by triggering the dissociation of cohesin complexes from chromosome arms, and all of these kinases are important for spindle assembly. The APC/C is essential for subsequent separation of sister chromatids and exit from mitosis. Precocious activation of the APC/C is prevented by a surveillance mechanism known as the spindle assembly checkpoint (SAC) (7), which inhibits the APC/C until all chromosomes have been properly bi-oriented. Once bi-orientation has been achieved, the SAC is inactivated. This enables the APC/C to initiate sister chromatid separation by activating separase, a protease that destroys sister chromatid cohesion by cleaving residual

<sup>1</sup>Research Institute of Molecular Pathology, Dr. Bohr-Gasse 7, 1030 Vienna, Austria. <sup>2</sup>Institute of Molecular Biotechnology of the Austrian Academy of Sciences, Dr. Bohr-Gasse 3, 1030 Vienna, Austria. <sup>3</sup>Departments of Biology and Biological Engineering, Koch Institute for Integrative Cancer Research, Massachusetts Institute of Technology, Cambridge, MA 02139, USA. <sup>4</sup>European Molecular Biology Laboratory, Meyerhofstrasse 1, 69117 Heidelberg, Germany. <sup>5</sup>Max Planck Institute for Molecular Cell Biology and Genetics, Pfotenhauerstrasse 108, 01307 Dresden, Germany. <sup>6</sup>Boehringer Ingelheim RCV GmbH & Co KG, Dr. Boehringer-Gasse 5-11, 1121 Vienna, Austria. <sup>7</sup>Department of Surgery, Beth Israel Deaconess Medical Center, Harvard Medical School, 330 Brookline Avenue, Boston, MA 02215, USA.

\*These authors contributed equally to this work.

†Present address: Institute of Biochemistry, Eidgenössische Technische Hochschule Zürich, Schafmattstrasse 18, CH-8093 Zürich, Switzerland.

‡Present address: CNRS Institute of Human Genetics, 141 rue de la Cardonille, 34396 Montpellier, France.

§Present address: Computation and Systems Biology, Singapore-MIT Alliance, 4 Engineering Drive 3, Singapore 117576, Republic of Singapore.

||To whom correspondence should be addressed. E-mail: peters@imp.ac.at

cohesin complexes on chromosomes. Both the chromosome segregation machinery and its regulatory enzymes are therefore essential for proper chromosome segregation.

Although chromosome segregation has long been known to depend on the ability of mitotic kinases to phosphorylate other proteins, it is poorly understood what the substrates of these enzymes are. Numerous large-scale mass spectrometric studies have, therefore, searched for proteins that are specifically phosphorylated during mitosis (8–13). These experiments have identified thousands of mitotic phosphorylation sites, but in most cases, it has not been determined which of these sites are generated by which kinase. Furthermore, none of these large-scale studies has systematically addressed how protein kinases target protein complexes. Therefore, we have used information obtained by the MitoCheck project (14) to identify mitotic phosphorylation sites on more than 100 purified human mitotic protein complexes. With the help of an algorithm refined for the detection of major mitotic kinase motifs (15), we predicted which phosphorylation sites are targeted by which kinase. To further explore these kinase dependencies for a subset of mitotic complexes, we used small-molecule inhibitors of AURKB [Hesperadin; (16)] and PLK1 (BI 4834; this study) in conjunction with tandem affinity protein purification and mass spectrometry (MS) with high sequence coverage (on average, 77% for bait proteins and their main interactors). We generated a set of phosphorylation-specific antibodies that directly confirmed that the generation of phosphorylation sites on these complexes depends on these kinases. Our results show that although most protein complexes required for chromosome segregation are phosphorylated on several complex subunits, in many cases one or two subunits are “hyperphosphorylated,” meaning that an unusually high number of phosphorylation sites exist on these proteins, and thus, these proteins might serve as “phosphate acceptors” for the phosphoregulation of the respective complex. Of the detected phosphorylation sites, we found that many were targeted by mitosis-specific protein kinases, but a considerable fraction depended on kinases that have so far not been associated with mitosis. Using the PLK1 and AURKB inhibitors, we identified sets of phosphorylation sites that depended on either or both of these kinases, with most proteins having only one or two sites dependent on these kinases. One marked exception is the cohesin subunit wings apart–like (WAPAL), on which we found that most of the phosphorylation sites are PLK1-dependent. Comparison of the kinase-dependent sites with the Scansite consensus motifs led to the identification of several high-confidence candidate substrates for PLK1 and AURKB in the following complexes: the cohesin complex, the RZZ [kinetochore-associated protein 1 (KNTC1, also known as rough deal, ROD), zeste white 10 (ZW10), ZWILCH] complex, the nucleoporin 107 (NUP107)–nucleoporin 160 (NUP160) complex, and the mitotic checkpoint complex (MCC).

## RESULTS

### Analysis of 107 mitotic protein complexes for the presence of phosphorylation sites

We previously characterized the intracellular location and subunit composition of 107 human protein complexes with various functions in mitosis (Fig. 1A) (14). Because numerous events in mitotic cells depend on mitotic protein kinases, we reasoned that many of these complexes might be phosphorylated during mitosis. To test this hypothesis and to establish a database of mitotic phosphorylation sites that in the future can be used for functional studies, we searched for phosphorylation sites in subunits of all of these complexes (Fig. 1B). We first analyzed the MS

data obtained for 1175 proteins that are components of these complexes (239 “bait” and 936 “prey” proteins) for the presence of phosphorylated peptides. All of these complexes were purified from HeLa cells arrested in mitosis (14). By applying the phosphosearch algorithm included in the Mascot software (17), we identified 1818 phosphorylation sites on 394

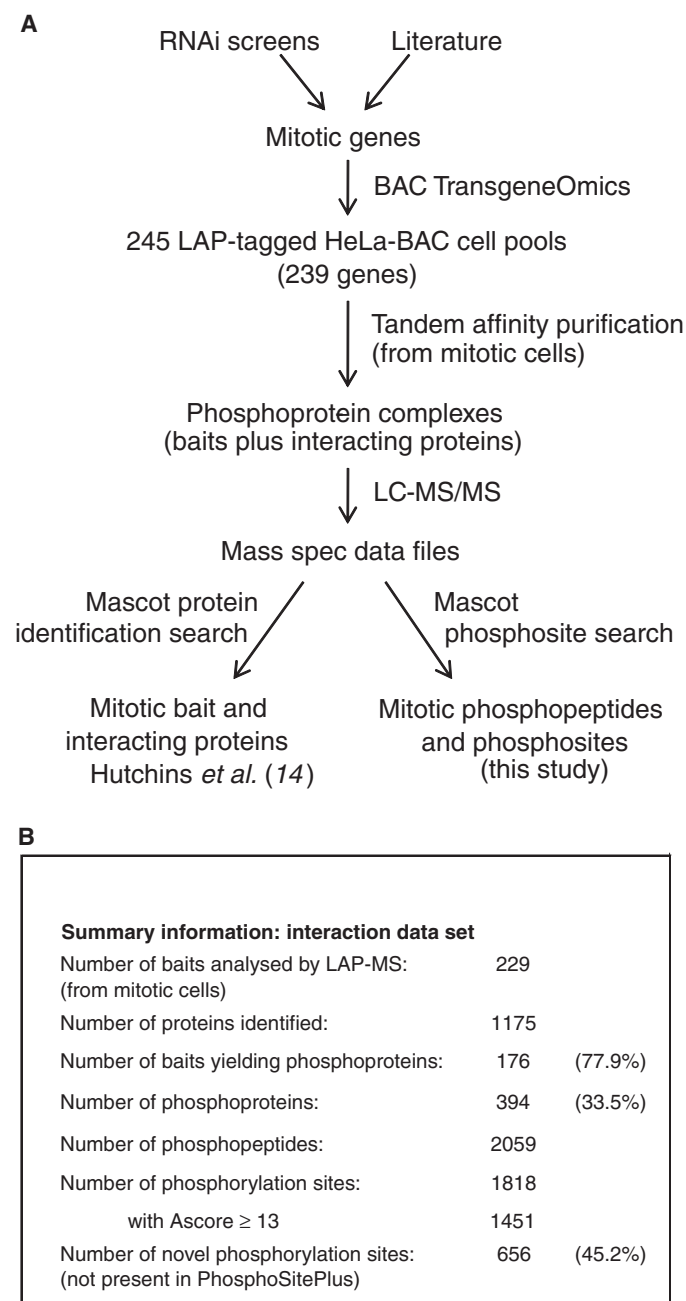


Fig. 1. Overview of the phosphorylation analysis of the mitotic interaction network. (A) Schematic outline of the workflow for mitotic gene selection, BAC tagging, phosphoprotein complex purification, and analysis. LC-MS/MS, liquid chromatography–tandem mass spectrometry. (B) Summary table of data obtained from the phosphorylation analysis of the mitotic interaction data set.

proteins (for a complete table of phosphorylated peptides and phosphorylation sites, see table S1). By using the Ascore algorithm (18), we could determine the precise position of the phosphorylated residue with a confidence above 95% (Ascore  $\geq 13$ ) for 1451 of these sites. Of these phosphorylation sites, 656 have not been previously reported in the public phosphorylation database PhosphoSitePlus (19). The 1451 phosphorylation sites that we identified were found on different subunits of 89 of the 107 different protein complexes (Fig. 2A), suggesting that most protein complexes with mitotic functions may be regulated by phosphorylation. As an example, the distribution of phosphorylation sites among subunits of 10 complexes is shown in Fig. 2B (see Cytoscape file S1 and fig. S1 for all complexes and tables S1 and S2 for a detailed listing of all phosphosites).

To test whether subunits of a given protein complex are phosphorylated to a similar extent, we determined the phosphorylation site density by calculating the number of sites per 100 amino acids actually detected by MS for each protein. Whereas the median phosphorylation site density was 1.07 sites per 100 amino acids across the whole data set (1.07% of 63,568 amino acids covered), analysis of all 26 complexes with 4 to 20 members showed that in 17 of those (65%) a few subunits per complex had a phosphorylation site density more than two times higher than the median of the entire complex (Fig. 2B, table S2, Cytoscape file S1, and fig. S1). For example, most APC/C subunits had a phosphorylation site density between 0.25% and 1.74% (APC/C median, 1.02%), whereas CDC23, CDC26, and CDC27 had a phosphorylation site density of about 3% (3.04%, 2.99%, 3.29%, respectively). These findings suggest that phosphoregulation of many protein complexes might be mediated by few subunits that function as “phosphoacceptors” and receive most of the kinase regulatory signal and possibly transmit this to other subunits in the complex.

To understand which kinases might phosphorylate these protein complexes, we analyzed the phosphorylation sites by applying the Scansite algorithm (15, 20, 21). Scansite uses position-specific scoring matrices (PSSMs) to predict which phosphorylation sites can be recognized by which of 32 different protein kinases. The PSSMs describe the relative preference of the kinases for residues upstream and downstream of the phosphorylation site as detected by incubating recombinant kinase with an oriented peptide library (22). Of the 1451 phosphorylation sites, 615 (42%) matched with high confidence (within the top 1.5% of Scansite hit scores) to 25 of the kinase motifs (Fig. 2C). More than a third of these phosphorylation sites (39%) are predicted to be targets of mitotic kinases: CDK1 [184 sites, subdivided into the CDK1 substrate subclasses identified by the Cdc2 (22), CDK1-1, and CDK1-2 motifs (15)], PLK1 (17 sites), AURKA (9 sites), AURKB (17 sites), and never in mitosis A (NIMA)-related protein kinase 2 (NEK2, 12 sites). To test whether any of the kinase motifs occurred more frequently in our set of mitotic protein complex phosphorylation sites than on average in the human proteome, we compared the frequency of these motifs in our data set with their frequency in the entire phosphoproteome as represented by the phosphorylation sites present in PhosphoSitePlus (19). This comparison revealed that the frequency of phosphorylation sites that match the motifs of CDK1, CDK5, ERK1 (extracellular signal-regulated kinase 1), and PKA (protein kinase A) was higher in our data set than would be predicted by a random distribution in the human proteome ( $P < 0.01$ ; fig. S2). Because the motifs of the proline-directed kinases CDK5 and ERK1 are similar to the motif recognized by CDK1 and because the PKA motif is similar to the motifs recognized by AURKA and AURKB, it is possible that the enrichment of the CDK5 and ERK1 motifs may be attributed to CDK1 activity, and the enrichment of the PKA motif may be attributed to the activity of AURKA and AURKB. These results indicate that most mitotic protein

complexes are controlled by phosphorylation, in many cases through multiple phosphorylation events on a few subunits, and that many of these modifications are generated by mitosis-specific protein kinases.

### Identification of phosphorylation sites sensitive to inhibitors of AURKB and PLK1 on 12 mitotic protein complexes

Although the analysis described above identified numerous phosphorylation sites, the analysis of the phosphorylation state of mitotic protein complexes remained incomplete because the average sequence coverage achieved in these experiments was only 38% per protein. Similar limitations apply to other large-scale phosphoproteomic studies in which similarly low sequence coverages have been obtained [see, for example, (11)]. Therefore, we selected a subset of 24 baits for high sequence coverage MS analysis that are subunits of 12 protein complexes with well-established essential functions in mitosis. We chose these complexes because knowledge of their phosphorylation states might be particularly valuable for understanding the regulation of mitosis. This subset includes complexes with functions in the SAC; at the kinetochore, including MCC, APC/C, nuclear division cycle 80 (NDC80), minichromosome loss 12 (MIS12), and associated proteins; and in chromosome segregation (cohesin and condensin), as well as regulators of the mitotic spindle [ $\gamma$ -tubulin ring complex ( $\gamma$ -TuRC), centralspindlin] and the mitotic kinases CDK1, PLK1, and AURKB (see Table 1 for a full list).

We identified the phosphorylation sites on these complexes and determined which of these phosphorylation sites were mitosis-specific and which mitosis-specific sites were sensitive to treatment with an inhibitor of AURKB or of PLK1, thus which of these sites might be dependent on the activities of these kinases in mitotic cells. We synchronized HeLa cells in four different states: in interphase by harvesting them under conditions where they were proliferating with a logarithmic proliferation curve (“LOG”), in mitosis by arresting them in prometaphase with nocodazole (“NOC”), or in mitosis where either AURKB activity was inhibited by treatment of the mitotic cells with the small-molecule inhibitor Hesperadin (“Hesp”) (16) or PLK1 activity was inhibited with a selective PLK1 inhibitor called BI 4834 (“BI”). In the Hesperadin experiments, cells were also treated with the proteasome inhibitor MG132 [*N*-(benzyloxycarbonyl)leucylleucylleucinal], because Hesperadin treatment would otherwise lead to rapid exit from mitosis (16). To confirm that the treatment of cells with nocodazole, BI 4834, or Hesperadin produced cells synchronized in prometaphase, we analyzed protein extracts from these cell populations by immunoblotting (Fig. 3A) and measurement of histone H1 kinase activity (Fig. 3B), which depends largely on CDK1 (23). As predicted, these experiments revealed an electrophoretic mobility shift of the APC/C subunit CDC27 and increased histone H1 kinase activity in the three cell populations treated with nocodazole and showed that BI 4834 did not inactivate AURKB activity, as measured by immunoblotting with antibodies specific to the activated phosphorylated form of AURKB (AURKB pThr<sup>232</sup>) and its substrate histone H3 (H3 pSer<sup>10</sup>), whereas these two phosphoepitopes were not detected in Hesperadin-treated cells (Fig. 3A).

For inhibition of PLK1, we used a novel small-molecule inhibitor, BI 4834, which is a dihydropteridinone derivative, similar in structure to BI 2536 (fig. S3A). This compound inhibits PLK1 [median inhibitory concentration (IC<sub>50</sub>), 7.6 nM] with higher selectivity than it exhibits for the related enzyme PLK3 (IC<sub>50</sub>, 198.4 nM), and this selectivity is greater than that of the previously characterized PLK1 inhibitor BI 2536 (24). To address whether the cellular phenotypes caused by BI 4834 are consistent with selective PLK1 inhibition, we released HeLa cells from a thymidine-induced S-phase arrest into media containing increasing doses of BI 4834 and analyzed fixed cells by immunofluorescence microscopy. At

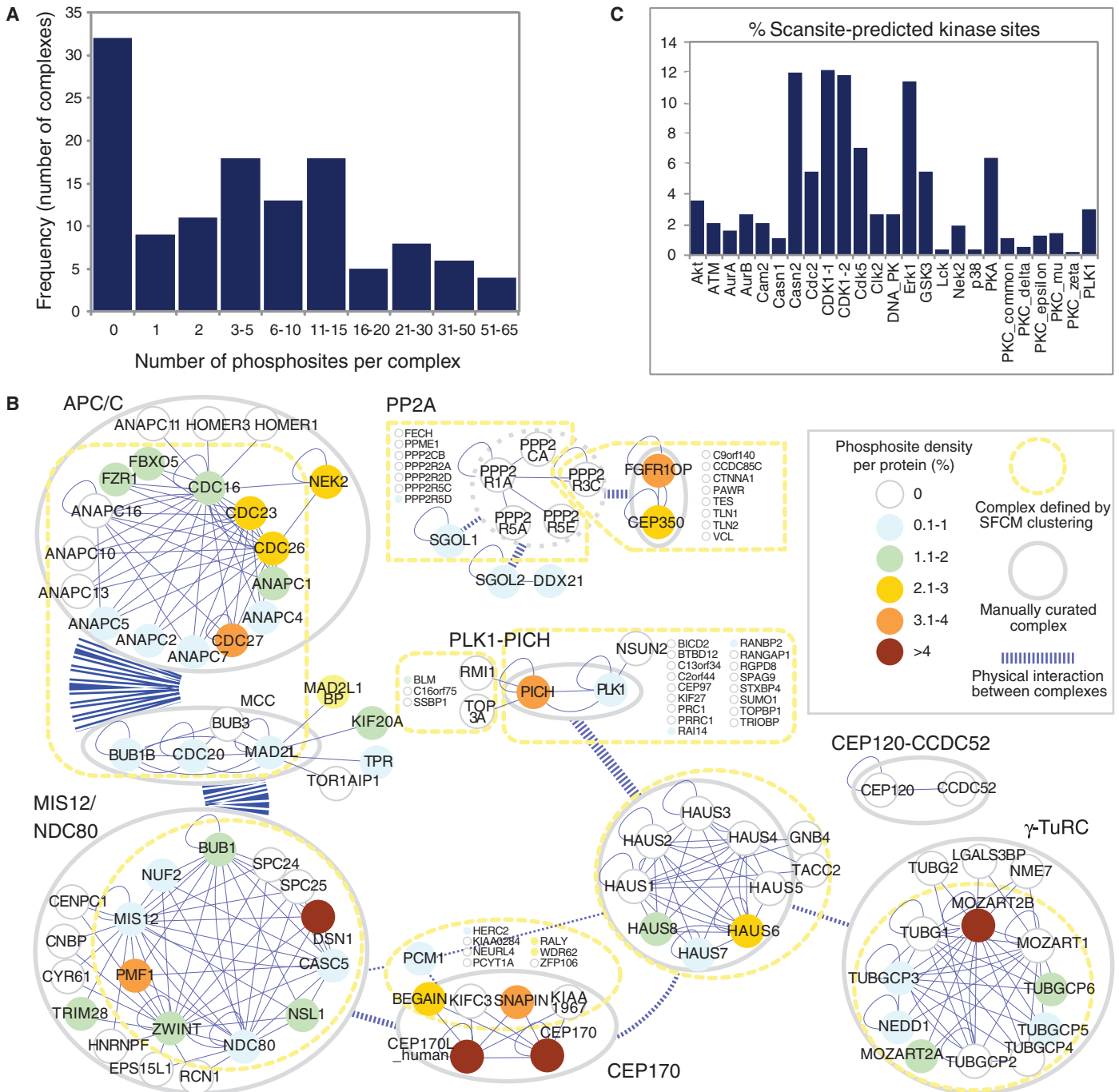


**Fig. 2.** Identification of phosphosites in proteins from the mitotic interaction network. **(A)** Frequency distribution graph of the number of phosphosites identified per interaction cluster in the mitotic interaction data set. **(B)** Interaction map for a selection of 9 of 107 small clusters as determined by spectral fuzzy *c*-means clustering [SFCM, described in (14)], showing the phosphorylation site density in percent for each protein. Complexes containing reciprocal interactions are enclosed by solid

gray lines; those without reciprocal interactions are denoted by dashed gray lines. Interactions between complexes are indicated by dashed blue lines with the number of interactions represented by line thickness. **(C)** Percent kinase motifs found within 615 high-confidence hits found in 1451 phosphorylation sites. Thirty-nine percent of all hits correspond to the mitotic kinases CDK1 (represented by three motif variants named Cdc2, CDK1-1, and CDK1-2), PLK1, AURKA, AURKB, and NEK2.

**Table 1.** Summary of complexes, baits (with their sequence coverage) and interactors, identified phosphoproteins, and phosphorylation sites in the four-condition data set. Sp, bait, the organism of the bait protein; Pf., purification method, Int., interactors; LOG, interphase; NOC, noc arrest; BI, noc arrest in combination with 2 hours of BI 4834; Hesp,

noc arrest in combination with a combination of Hesperadin and MG132; Ph proteins, the number of phosphorylated proteins; Ph sites, the number of phosphorylated sites; CPC, chromosomal passenger complex [AURKB, INCENP, baculoviral IAP repeat-containing protein 5 (BIRC5), CDCA8]; na, purification not performed.

Complex	Sp. bait	Bait	Pf.	Int.	% Seq. coverage bait				Ph proteins	Ph sites
					LOG	NOC	BI	Hesp		
Dynactin	Mm	Actr1a	LAP	5	93	94	93	96	1	6
γ-TuRC	Mm	Tubg1	LAP	96	96	93	94	92	4	14
CPC	Mm	Aurkb	LAP	13	77	79	78	81	4	43
CDK1	Mm	Cdk1	LAP	9	78	84	82	88	5	7
PLK1	Mm	PLK1	LAP	9	72	34	36	74	3	4
MIS12/NDC80	Mm	Bub1	LAP	25	84	89	89	88	8	41
MIS12/NDC80	Mm	Mis12	LAP	30	84	74	81	83	7	26
MIS12/NDC80	Hs	NSL1	Ab	65	78	67	na	na	4	19
RZZ	Mm	Zw10	LAP	23	85	85	84	85	4	13
MCC	Mm	Bub1b	LAP	55	83	86	86	89	13	49
MCC	Mm	Mad2l1	LAP	105	98	95	93	95	6	30
APC/C	Hs	CDC27	Ab	64	87	78	81	94	17	124
NUP107-160	Mm	Nup107	LAP	39	82	87	86	12	6	53
Centralspindlin	Mm	Kif23	LAP	7	31	36	37	47	5	23
Centralspindlin	Mm	Racgap1	LAP	9	58	57	61	54	7	64
Cohesin	Mm	Cdca5	LAP	23	78	75	65	66	1	8
Cohesin	Hs	PDS5A	Ab	238	76	91	64	80	4	27
Cohesin	Hs	PDS5B	Ab	42	81	75	58	73	3	26
Cohesin	Hs	STAG1	Ab	298	65	69	na	na	6	18
Cohesin	Hs	STAG2	Ab	243	60	78	74	72	11	53
Cohesin	Hs	WAPAL	Ab	27	19	68	77	31	5	32
Condensin-I	Hs	NCAPH	FLAG	6	20	18	0	22	4	19
Condensin-II	Hs	NCAPH2	FLAG	7	0	10	0	0	2	6
SMC5/6	Mm	Smc6	LAP	40	42	43	43	42	5	19
Mean					78	76	77	77		

BI 4834 concentrations between 250 and 500 nM, more than 85% of all cells arrested in prometaphase with monopolar spindles (“Polo phenotype”; fig. S3, B and C) and with reduced amounts of tubulin γ 1 (TUBG1) at centrosomes (fig. S3, D and E). BI 4834 treatment also reduced the centrosomal signal of a PLK1-dependent phosphoepitope on the APC/C subunit cell division cycle 16 (CDC16 pSer<sup>560</sup>) (25) (fig. S3F) and reduced the dissociation of cohesin from chromosome arms (fig. S3G). Western blot analysis revealed that BI 4834 treatment abolished the electrophoretic mobility shifts of budding uninhibited by benzimidazoles 1B (BUB1B) and CDC25C, which depend on PLK1 (fig. S3H) (24, 26). All of these observations are consistent with inactivation of PLK1, indicating that the cellular phenotype caused by BI 4834 is primarily the result of PLK1 inhibition.

We isolated all 24 baits and their interactors from cells cultured under four conditions (LOG, NOC, BI, and Hesp). The baits were purified from HeLa cells stably expressing the bait protein from a bacterial artificial chromosome (BAC), by using a localization and affinity purification (LAP) tag (27) for tandem affinity purification (TAP) (14, 28), or in a few cases by immunoprecipitation with bait-specific antibodies. In some cases, mouse proteins were used as baits because HeLa cells containing the corresponding mouse BACs had previously been used to test the functionality of the LAP-tagged bait proteins in RNA interference (RNAi) “rescue” experiments (14, 28, 29). Of each of the resulting 96 protein isolates, we analyzed a small fraction by SDS-PAGE (polyacrylamide gel electrophoresis) and silver staining to assess their purity, subjected the remainder to digestion with three different proteases, and identified phosphopeptides in each of the resulting 288 samples (Fig. 3, C and D). This procedure resulted in a high sequence coverage for the bait proteins and their main in-

teractors [on average 77% (Table 1)] and in a total of 1183 phosphorylation sites. All phosphosites were validated by manual inspection of the corresponding MS spectra and were rated according to a quality score (see Materials and Methods and fig. S4). Spectra of poor quality (score 0) were excluded from the analysis. For 615 sites of high quality, the position of the phosphorylated residue could be determined unambiguously, and 457 of these sites were covered by peptides in all four experimental conditions (either in their phosphorylated or in their unphosphorylated form, depending on the experimental condition). Phosphorylation sites that were not covered in all four conditions were excluded from the subsequent comparison.

Of the 457 phosphorylation sites, only 21 sites were specifically phosphorylated in cells in interphase; the phosphorylated peptides covering these sites were only found in the LOG sample, whereas only unphosphorylated peptides covering these sites were found in the other three conditions. Conversely, 400 sites were found phosphorylated in mitotic cells (NOC, table S3). We analyzed these mitotic phosphorylation sites with the Scansite algorithm containing motifs of 32 kinases. Of the 400 sites, 300 matched to the PSSM of one of 24 protein kinases (Fig. 3E). Similarly to what we found in the Scansite analysis of the large-scale interaction data set (Fig. 2C), one-third of all phosphorylation sites (34%) was predicted as targets of mitotic kinases, including PLK1 (16 sites, 5.3%) and AURKB (7 sites, 2.3%).

Because in this data set the sequence coverage of the analyzed protein complexes is higher than in the interaction data set (see Fig. 4, A and B, for a representative purification), we wanted to test the observation that most complexes are hyperphosphorylated on only one or two of their subunits. The median phosphorylation site density was 1.4 sites per 100 amino acids

covered (1.4% of 40,082 amino acids covered) across all 12 analyzed complexes. In 8 of these complexes (67%), one or two subunits per complex had a phosphorylation site density more than two times higher than the median of the entire complex (Fig. 4C and table S4). These

data thus confirm the finding from the interaction data set, and strengthen the hypothesis that a few subunits within a complex might act as target sites for various kinases to mediate phosphoregulation of a protein complex.

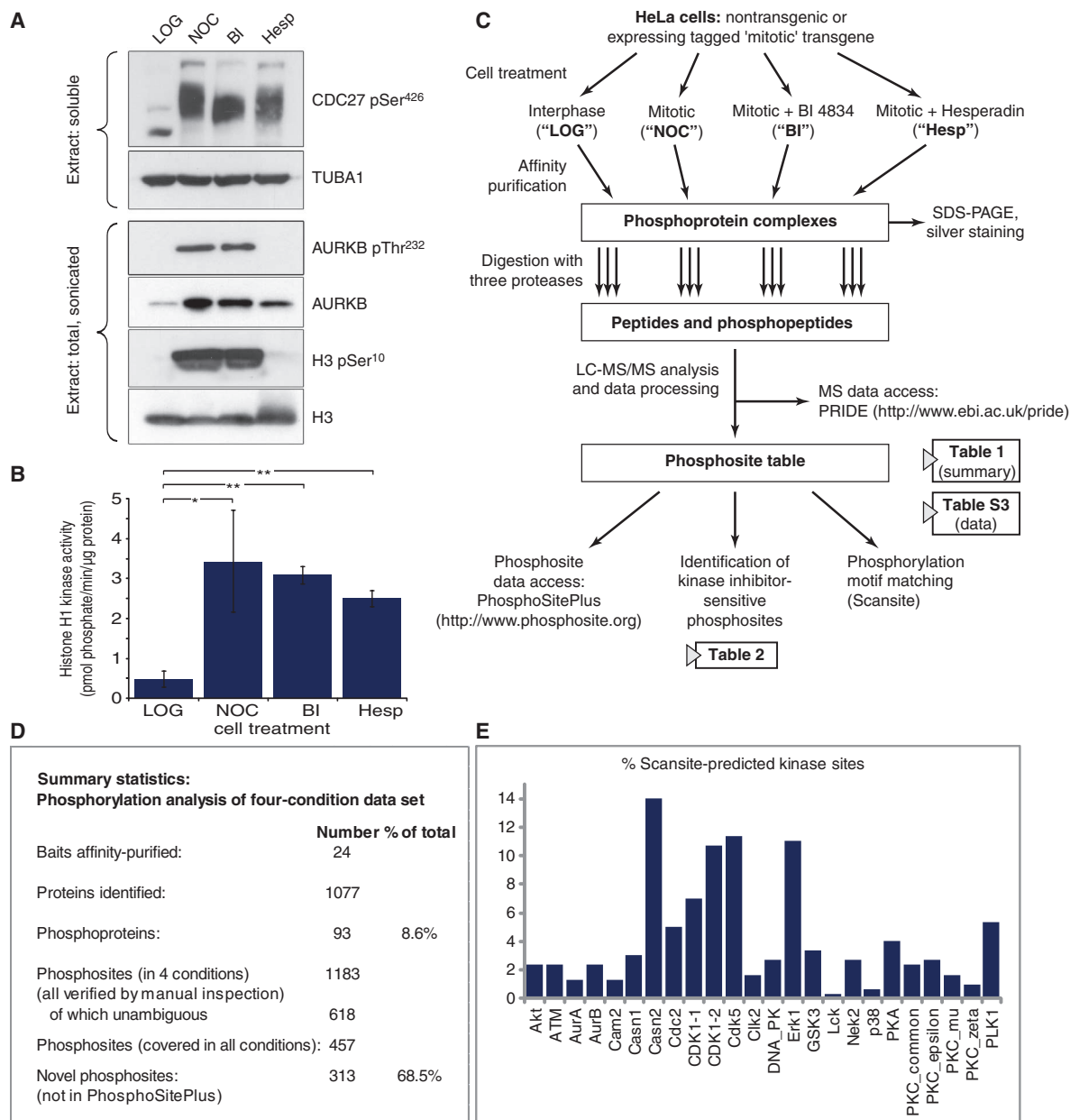


**Fig. 3.** Experimental conditions for the identification of mitosis-specific and kinase inhibitor-sensitive phosphorylation sites. (A) Western blots of cell extracts from the four conditions described in (C) probed with the indicated antibodies (representative of two experiments). (B) Histone H1 kinase activities of cell extracts from the conditions described in (C). Assays were performed on four samples per condition ( $n = 4$ ); error bars represent SD.  $*P \leq 0.05$ ;  $**P \leq 0.005$ , determined by Student's  $t$  test (77). (C) Scheme of the workflow for purification of phosphoprotein complexes and data analysis of four conditions: LOG, interphase; NOC, 18 hours of nocodazole

arrest; BI, 18 hours of nocodazole arrest with additional treatment of 250 nM BI 4834 for the last 2 hours; Hesp, 18 hours of nocodazole arrest with additional treatment of 100 nM Hesperadin and 10  $\mu$ M MG132 for the last 2 hours. (D) Summary table of data obtained from phosphorylation analysis of 24 baits from samples as described in (C). (E) Percent kinase motifs found within 455 high-confidence hits found in 618 phosphorylation sites. Thirty-three percent of all hits correspond to the mitotic kinases CDK1 (represented by three motif variants named Cdc2, CDK1-1, and CDK1-2), PLK1, AURKA, AURKB, and NEK2.

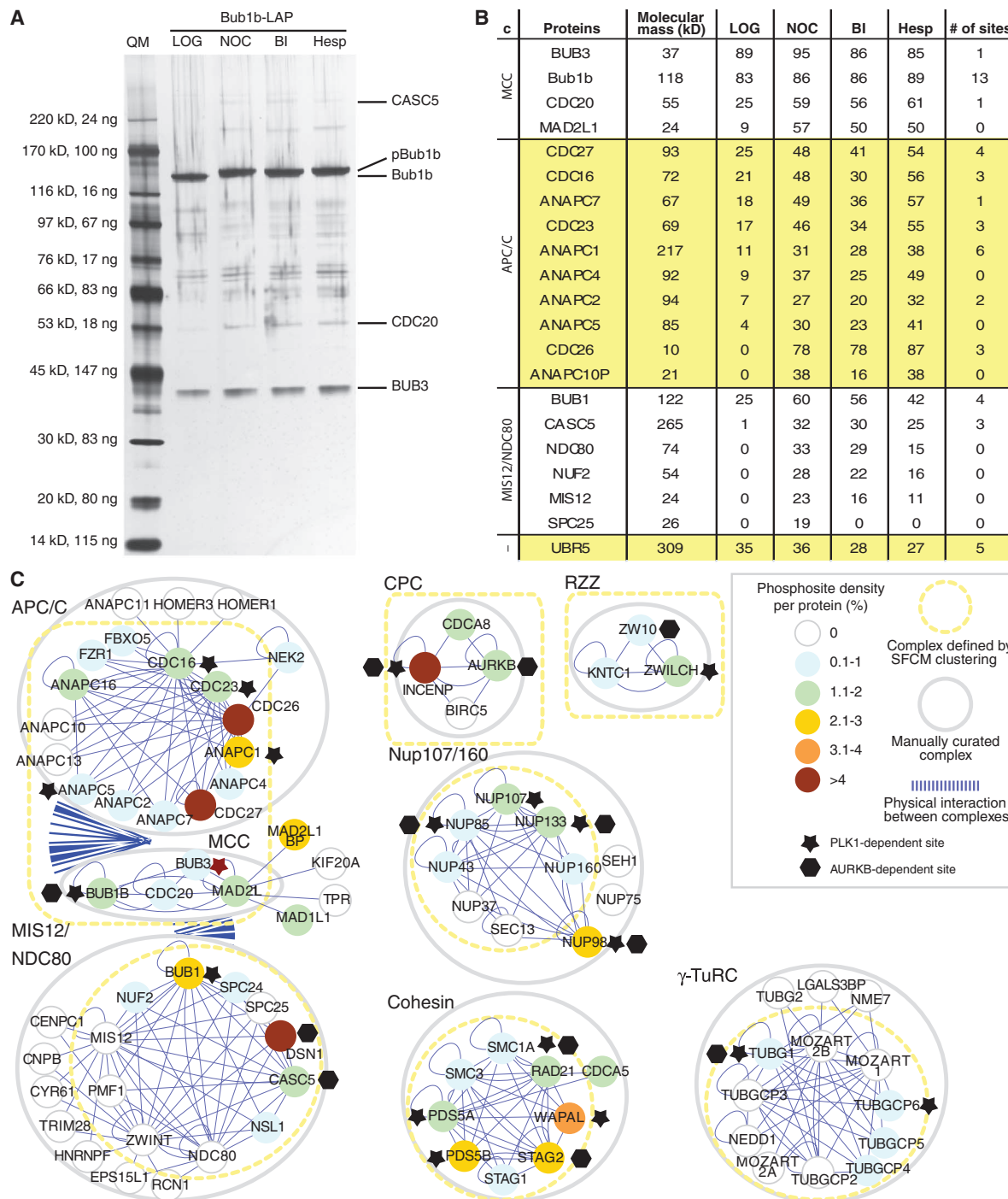


**Fig. 4.** Identification of phosphorylation sites in protein complexes from the four-condition data set. (A) Silver-stained SDS-PAGE gel showing proteins purified from the four cell-treatment conditions (LOG, NOC, BI, Hesp) after a LAP-TAP purification with mouse Bub1b as bait. This gel illustrates the level of purity achieved in purifications carried out with 24 different baits. Annotated protein bands are based on their expected migration positions; the intensity of the marker bands corresponds to the annotated protein amounts in nanograms. (B) Phosphoproteins and phosphosites identified by MS analysis of the three protein complexes MCC, APC/C,

and MIS12/NDC80 and the co-purifying protein UBR5; the first column (c) indicates complex membership, affinity-purified with the mouse Bub1b-LAP bait from the four conditions, as shown in (A). The percentages result from the sequence coverages obtained after combining peptides generated by all proteases. (C) Interaction map for a selection of 8 of 12 complexes analyzed in the four treatment conditions, projected onto the interaction clusters determined by Hutchins *et al.* (14), showing the phosphorylation site density (in percent) for each protein and indicating proteins with sites dependent on PLK1 and AURKB.

To determine experimentally which of the 400 mitotic phosphorylation sites were dependent on PLK1 or AURKB *in vivo*, we compared which phosphorylation sites were lost in samples from cells treated with BI 4834 or Hesperadin. In BI 4834-treated cells, 96 phosphorylation sites on 35 proteins could not be detected, and treatment of cells with Hesperadin resulted in the absence of 74 sites on 32 proteins, even though the corresponding nonphosphorylated peptides were recovered in all cases. Between these two treatments, 54 phosphorylation sites were overlapping, suggesting that these were indirectly dependent on PLK1 and AURKB activity. We, thus, identified 42 phosphorylation sites in 25 proteins (14% of all mitotic sites) that were dependent only on PLK1 and 20 phosphorylation sites in 18 proteins (5% of all mitotic sites) that were dependent only on AURKB (see Fig. 4C for a graphical representation and Table 2 for a summary of all identified sites and proteins). Because we had treated the cells with kinase inhibitors for 2 hours, it is likely that some of the phosphorylation sites that we identified as kinase-dependent are not direct substrates of the inhibited kinases. To identify proteins that might be direct PLK1 or AURKB substrates, we used the newly developed PLK1 and AURKB PSSMs in Scansite (15). Among the 42 experimentally determined BI 4834-sensitive sites were 11 residues (located on eight proteins) predicted by Scansite to be PLK1 targets (Table 2, sites in bold). Five of these proteins [NUP107, radiation-sensitive 21 (RAD21), stromal antigen 2 (STAG2), WAPAL, and ZWILCH] are previously unknown PLK1 substrates, whereas the other three [BUB1, BUB1B, and mitotic arrest deficient-like 1 (MAD1L1)] are known PLK1 substrates (26, 30, 31). However, experimental evidence for the PLK1-dependent phosphorylation of these 11 sites had not been previously reported. Among the 20 Hesperadin-sensitive sites were three residues (located on three proteins) predicted by Scansite to be AURKB targets (Table 2, sites in bold). One protein, RAD21, is a previously unknown AURKB substrate, whereas the other two [chromobox protein homolog 5 (CBX5), inner centromere protein (INCENP)] are known AURKB substrates (32–34). Two of the three sites (on RAD21 and CBX5) were previously not known to depend on AURKB. The combination of the *in silico* Scansite predictions with our *in vivo* inhibitor results thus identifies one previously unknown, high-confidence substrate candidate for AURKB and five for PLK1.

### Validation of selected phosphorylation sites by phosphospecific antibodies

Because our analysis of the dependence of phosphorylation sites on PLK1 and AURKB was, in part, based on negative evidence, the absence of phosphorylated peptides in certain experimental conditions, we generated phosphospecific antibodies to 13 of the identified phosphorylation sites. We used these antibodies to validate the MS data in immunoblotting experiments, using either whole-cell extracts or, in cases where the antibodies were not sensitive enough to detect their antigen in such extracts, immunoprecipitated proteins. We raised four antibodies to BI 4834-sensitive sites that had been identified on the cohesin subunits STAG2 (Ser<sup>1261</sup>) and WAPAL (Ser<sup>465</sup>, Ser<sup>528</sup>, and Ser<sup>1154</sup>). Immunoblot analysis of cell extracts or WAPAL immunoprecipitates (Fig. 5A) confirmed that the phosphorylation of all four sites was inhibited by BI 4834. When STAG2 or WAPAL immunoprecipitates obtained from interphase cells were incubated with purified PLK1 and ATP (adenosine 5'-triphosphate), the phosphorylated forms of these proteins that were recognized by the corresponding phosphorylation-specific antibodies could be generated *in vitro* (Fig. 5B), consistent with the possibility that these sites are direct substrates of PLK1. The Ser<sup>1261</sup> site on STAG2 and the Ser<sup>465</sup> site on WAPAL were also predicted by Scansite to be PLK1 targets; the *in vitro* kinase assays thus confirmed these *in silico* predictions. In the case of STAG2, immunofluorescence microscopy experiments further

supported the notion that phosphorylation of Ser<sup>1261</sup> is mediated by PLK1, because the mitotic staining obtained with pSer<sup>1261</sup> antibodies was largely abolished by treatment of cells with BI 4834 (Fig. 5C).

We also generated antibodies to Hesperadin-sensitive sites on the AURKB interactor INCENP (residue Ser<sup>446</sup>), the nucleoporin NUP85 (Thr<sup>90</sup>), BUB1B (Ser<sup>551</sup>), and the condensin subunit non-SMC (structural maintenance of chromosomes) chromosome-associated protein D2 (NCAPD2). For NCAPD2, the position of the phosphorylated residue could not be unambiguously identified, and antibodies were, therefore, raised against both potential sites (Thr<sup>1388</sup> and Thr<sup>1389</sup>). Immunoblot analysis of NUP85 purified by TAP of its interaction partner NUP107 and of INCENP in cell extracts (Fig. 5D) confirmed that the chosen phosphorylation sites on these proteins were sensitive to Hesperadin treatment, whereas no Hesperadin sensitivity could be observed when BUB1B immunoprecipitates were analyzed by immunoblotting with the corresponding phosphospecific antibodies. The two antibodies raised against sites on NCAPD2 could both recognize NCAPD2 in mitotic but not in interphase extracts (Fig. 5D), consistent with the possibility that NCAPD2 can be phosphorylated on either Thr<sup>1388</sup>, Thr<sup>1389</sup>, or both, but these reactions were not decreased in cells treated with Hesperadin (for a summary of all results obtained with the phosphospecific antibodies, see Fig. 5E).

Finally, we raised one antibody to a site on the cohesin subunit precocious dissociation of sisters 5A (PDS5A, residue Ser<sup>1233</sup>) that was mitosis-specific but not inhibited by either BI 4834 or Hesperadin, and to four sites on the cohesin subunits RAD21 (Ser<sup>153</sup>, Ser<sup>175</sup>) and PDS5B (Ser<sup>1384</sup>, Ser<sup>1418</sup>) that had been found in all experimental conditions. Immunoblot analysis of the corresponding immunoprecipitates confirmed that the PDS5A site was mitosis-specific and that the two sites on PDS5B were present in interphase and mitosis (fig. S5A). However, the two sites on RAD21 were found to be mitosis-specific and sensitive to BI 4834 treatment (fig. S5, A and B).

In summary, the MS data for four of the four tested BI 4834-sensitive sites, two of four Hesperadin-sensitive sites, one of one mitosis-specific site, and two of four unregulated sites, in total 9 of 13 sites, were confirmed by experiments with phosphospecific antibodies. In the remaining four cases, it is possible that the MS data were insufficient to determine the abundance change of these phosphorylation sites. These results indicate that most of the obtained MS data are reliable for a given phosphorylation site that is sensitive to BI 4834 or Hesperadin. Our MS experiments have, therefore, identified a large number of previously unknown candidate substrates of PLK1 and AURKB among human protein complexes essential for mitosis.

### Data availability

These data complement the protein interaction study of Hutchins *et al.* (14). Phosphosites from this study have been incorporated into the PhosphoSitePlus (<http://www.phosphosite.org>) (19) and Phospho.ELM (<http://phospho.elm.eu.org>) (35) databases. Interpreted phosphopeptide spectrum data are accessible through the PRoteomics IDentifications database (PRIDE, <http://www.ebi.ac.uk/pride/>) (36), and raw MS data files are available for download; see table S5 for details.

### DISCUSSION

Oscillatory protein phosphorylation regulates the major phase transitions of the cell division cycle. The overall amount of phosphorylation is especially high during mitosis (37, 38), and several large-scale studies have identified sets of phosphorylation sites present during mitosis (8, 11–13, 39). These studies, although mostly performed on a “phosphoproteome” scale, are still far from complete due to the complexity and variance in protein abundance within the proteome (40). Because phosphoproteomic studies

# RESEARCH RESOURCE

usually rely on phosphopeptide enrichment, the information about the unphosphorylated proteins is lost, and it thus remains difficult to estimate the protein coverage in these studies. Here, we have taken a complementary approach to analyze mitotic phosphorylation within purified mitotic protein complexes. The much lower sample complexity allowed simultaneous analysis of phosphorylated and unphosphorylated peptides to obtain a measure of sequence coverage for each analyzed protein and protein complex. After the development of high-throughput tagging and protein purification for human cells within the MitoCheck project (14, 28), we

have systematically analyzed 107 mitotic protein complexes for protein phosphorylation. We identified a set of 1451 phosphorylation sites on 89 complexes, indicating that most mitotic protein complexes become phosphorylated in mitosis.

This large data set on the phosphorylation of protein complexes allowed us to address how phosphorylation sites are distributed within protein complexes. We found that, in many cases, only one or two subunits carry most of the phosphorylation sites of the whole complex (Figs. 2B and 4C and Cytoscape file S1). This finding is consistent with phosphorylation site

**Table 2.** Summary of proteins identified containing PLK1- or AURKB-dependent phosphorylation sites, with sites matching Scansite sequence motifs in bold. Sp. bait, the organism of the bait protein; Mit. sites, mitotic sites; BI-sens, all sites sensitive to BI 4834 treatment; BI

only, all BI-sensitive sites that are not also sensitive to Hesperadin treatment; Hesp-sens, all sites sensitive to Hesperadin treatment; Hesp only, all Hesp-sensitive sites that are not also sensitive to BI 4834 treatment.

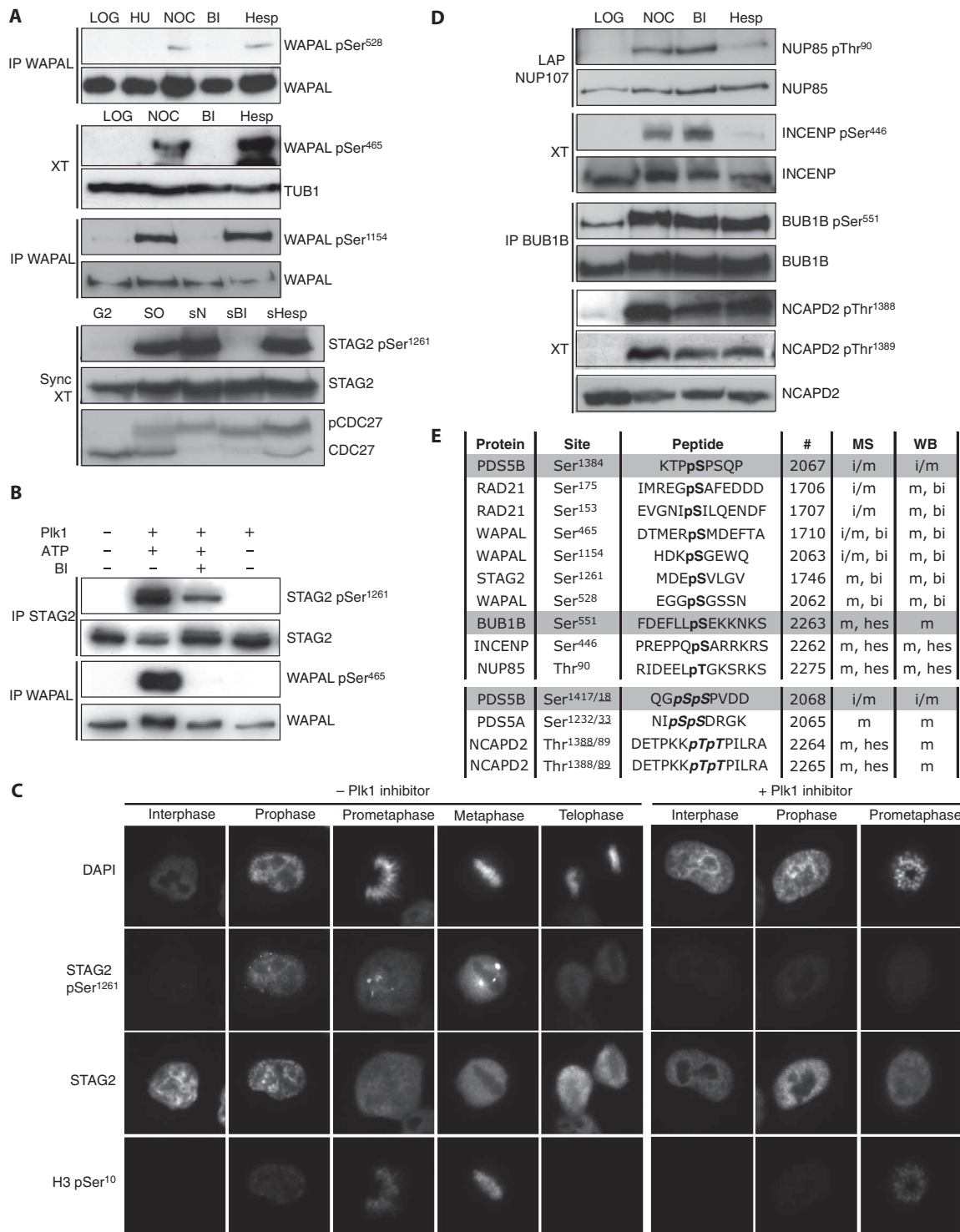
Complex	Sp	Name	Mit. sites	BI-sens. (BI only)	Hesp-sens (Hesp only)	BI-sens. sites	Hesp-sens. sites
γ-TuRC	Mm	Tubg1	3	2 (1)	2 (1)	Ser <sup>131</sup> , Ser <sup>32</sup>	Ser <sup>284</sup> , Ser <sup>32</sup>
γ-TuRC	Hs	TUBGCP6	5	1 (1)	0	Ser <sup>242</sup>	—
CPC	Mm	Aurkb	4	2 (0)	3 (1)	Ser <sup>71</sup> , Ser <sup>25</sup>	Ser <sup>71</sup> , Thr <sup>237</sup> , Ser <sup>25</sup>
CPC	Hs	CDCA8	3	2 (0)	2 (0)	Thr <sup>185</sup> , Thr <sup>106</sup>	Thr <sup>185</sup> , Thr <sup>106</sup>
CPC	Hs	INCENP	29	9 (5)	5 (1)	Thr <sup>832</sup> , Ser <sup>894</sup> , Ser <sup>893</sup> , Ser <sup>914</sup> , Thr <sup>239</sup> , Thr <sup>507</sup> , Thr <sup>145</sup> , Ser <sup>828</sup> , Ser <sup>831</sup>	Ser <sup>894</sup> , Ser <sup>893</sup> , Thr <sup>507</sup> , Ser <sup>914</sup> , Ser <sup>446</sup>
CDK1	Mm	Cdk1	3	0	1 (1)	—	Tyr <sup>15</sup>
PLK1	Mm	Plk1	2	1 (1)	0	Ser <sup>331</sup>	—
MIS12/NDC80	Mm	Bub1	12	4 (2)	2 (0)	Ser <sup>689</sup> , Ser <sup>387</sup> , Ser <sup>321</sup> , Ser <sup>400</sup>	Ser <sup>689</sup> , Ser <sup>387</sup>
MIS12/NDC80	Hs	CASC5	8	2 (0)	5 (3)	Ser <sup>633</sup> , Ser <sup>1675</sup>	Thr <sup>513</sup> , Ser <sup>633</sup> , Ser <sup>1675</sup> , Thr <sup>517</sup> , Ser <sup>32</sup>
MIS12/NDC80	Hs	DSN1	8	0	1 (1)	—	Ser <sup>41</sup>
RZZ	Mm	Zw10	3	0	1 (1)	—	Ser <sup>755</sup>
RZZ	Hs	ZWILCH	7	3 (2)	1 (0)	Ser <sup>565</sup> , Ser <sup>75</sup> , Thr <sup>74</sup>	Ser <sup>565</sup>
MCC	Mm	Bub1b	10	2 (2)	1 (1)	Ser <sup>529</sup> , Ser <sup>527</sup>	Thr <sup>601</sup>
MCC	Hs	BUB1B	7	2 (1)	2 (1)	Ser <sup>747</sup> , Ser <sup>381</sup>	Ser <sup>747</sup> , Ser <sup>551</sup>
MCC	Hs	BUB3	2	1 (1)	0	Ser <sup>211</sup>	—
APC/C	Hs	ANAPC1	16	3 (1)	2 (0)	Thr <sup>530</sup> , Ser <sup>333</sup> , Ser <sup>362</sup>	Ser <sup>333</sup> , Ser <sup>362</sup>
APC/C	Hs	ANAPC5	5	4 (2)	2 (0)	Ser <sup>179</sup> , Thr <sup>178</sup> , Ser <sup>195</sup> , Ser <sup>221</sup>	Ser <sup>179</sup> , Ser <sup>195</sup>
APC/C	Hs	ANAPC7	2	1 (0)	1 (0)	Ser <sup>125</sup>	Ser <sup>125</sup>
APC/C	Hs	CDC16	3	1 (1)	0	Ser <sup>112</sup>	—
APC/C	Hs	CDC23	8	2 (2)	0	Ser <sup>576</sup> , Ser <sup>593</sup>	—
APC/C	Hs	CDC27	12	1 (1)	0	Ser <sup>220</sup>	—
NUP107-160	Mm	Nup107	12	5 (0)	5 (0)	Ser <sup>68</sup> , Ser <sup>653</sup> , Thr <sup>784</sup> , Ser <sup>4</sup> , Ser <sup>138</sup>	Ser <sup>653</sup> , Ser <sup>68</sup> , Thr <sup>784</sup> , Ser <sup>4</sup> , Ser <sup>138</sup>
NUP107-160	Hs	NUP133	11	1 (1)	1 (1)	Thr <sup>512</sup>	Ser <sup>72</sup>
NUP107-160	Hs	NUP85	2	1 (1)	1 (1)	Ser <sup>223</sup>	Thr <sup>90</sup>
NUP107-160	Hs	NUP98	15	4 (3)	2 (1)	Ser <sup>949</sup> , Ser <sup>931</sup> , Ser <sup>1006</sup> , Thr <sup>983</sup>	Ser <sup>1448</sup> , Ser <sup>931</sup>
Cohesin	Hs	PDS5A	13	6 (1)	5 (0)	Ser <sup>870</sup> , Ser <sup>865</sup> , Ser <sup>1177</sup> , Ser <sup>1097</sup> , Thr <sup>1178</sup> , Ser <sup>1172</sup>	Ser <sup>870</sup> , Ser <sup>1177</sup> , Ser <sup>865</sup> , Thr <sup>1178</sup> , Ser <sup>1172</sup>
Cohesin	Hs	PDS5B	16	4 (1)	3 (0)	Ser <sup>1165</sup> , Ser <sup>1319</sup> , Ser <sup>1162</sup> , Thr <sup>1301</sup>	Ser <sup>1165</sup> , Ser <sup>1162</sup> , Ser <sup>1319</sup>
Cohesin	Hs	RAD21	8	4 (2)	3 (1)	Ser <sup>134</sup> , Thr <sup>623</sup> , Ser <sup>545</sup> , Ser <sup>138</sup>	Thr <sup>366</sup> , Ser <sup>134</sup> , Ser <sup>545</sup>
Cohesin	Hs	SMC1A	2	1 (0)	1 (0)	Ser <sup>735</sup>	Ser <sup>735</sup>
Cohesin	Hs	SMC3	2	1 (0)	1 (0)	Ser <sup>85</sup>	Ser <sup>85</sup>
Cohesin	Hs	STAG2	12	9 (1)	9 (1)	Ser <sup>1091</sup> , Ser <sup>752</sup> , Thr <sup>1124</sup> , Ser <sup>1261</sup> , Thr <sup>1151</sup> , Thr <sup>1146</sup> , Ser <sup>1137</sup> , Ser <sup>1140</sup> , Ser <sup>751</sup>	Ser <sup>843</sup> , Ser <sup>1091</sup> , Ser <sup>752</sup> , Thr <sup>1124</sup> , Ser <sup>1261</sup> , Thr <sup>1151</sup> , Thr <sup>1146</sup> , Ser <sup>1137</sup> , Ser <sup>1140</sup> , Ser <sup>751</sup>
Cohesin	Hs	WAPAL	20	10 (7)	3 (0)	Ser <sup>505</sup> , Ser <sup>1154</sup> , Ser <sup>989</sup> , Thr <sup>276</sup> , Ser <sup>1161</sup> , Ser <sup>465</sup> , Ser <sup>629</sup> , Ser <sup>528</sup> , Ser <sup>371</sup> , Thr <sup>1160</sup>	Ser <sup>505</sup> , Thr <sup>276</sup> , Thr <sup>1160</sup>
Condensin	Hs	NCAPD2	2	0	1 (1)	—	Thr <sup>1388/1389</sup>
SMC5/6	Hs	NSMCE4A	4	1 (1)	0	Thr <sup>58</sup>	—
SMC5/6	Hs	SMC5	2	0	1 (1)	—	Ser <sup>12</sup>
—	Hs	CBX5	1	1 (0)	1 (0)	Ser <sup>92</sup>	Ser <sup>92</sup>
—	Hs	KIF2C	4	2 (0)	2 (0)	Ser <sup>633</sup> , Ser <sup>166</sup>	Ser <sup>633</sup> , Ser <sup>166</sup>
—	Hs	MAD1L1	8	1 (1)	1 (1)	Ser <sup>490</sup>	Ser <sup>551</sup>
—	Hs	MAD2L1BP	1	1 (0)	1 (0)	Ser <sup>42</sup>	Ser <sup>42</sup>
—	Hs	MAD2L1BP	2	1 (1)	0	Ser <sup>78</sup>	—
—	Hs	UBR5	4	1 (0)	2 (1)	Ser <sup>327</sup>	Ser <sup>110</sup> , Ser <sup>327</sup>
Total				96 (42)	74 (20)	35 (25)	32 (18)

Downloaded from [stke.sciencemag.org](http://stke.sciencemag.org) on December 29, 2011

analyses of the APC/C and cohesin complexes (9, 25, 41, 42). In combination with available structural and functional data for some of these complexes, our data suggest that hyperphosphorylated subunits might

serve as phosphate acceptors that relay phosphoregulatory signals within the protein complex. For example, the tetratricopeptide repeat (TPR) subunits of the APC/C (CDC16, CDC23, and CDC27) were shown by electron

**Fig. 5.** Phosphospecific antibodies validate MS results. **(A)** Phosphospecific antibodies [listed in (E)] were tested on cell extract (XT) or immunopurified protein (IP). XT were from interphase (LOG), noc arrest (NOC), and noc arrest in combination with 2 hours of BI 4834 (BI) or a combination of Hesperadin and MG132 (Hesp). The STAG2 pSer<sup>1261</sup> antibody was tested on XT from synchronized cells harvested either in G<sub>2</sub>, in mitosis by shake-off (SO), in mitosis with 3 hours of nocodazole treatment (sN), or in mitosis with 3 hours of nocodazole and the last 2 hours either in BI 4834 (sBI) or in Hesperadin plus MG132 (sHesp). Cell cycle stage was verified with the indicated antibodies. *n* = 2 experiments. **(B)** STAG2 and WAPAL were immunopurified from LOG and incubated with PLK1, ATP, and 1 μM BI 2536. Western blots were performed with the indicated antibodies. *n* = 2 experiments. **(C)** Immunofluorescence images of cells at different cell cycle stages treated or not with 100 nM BI 2536 for 30 min before fixation were stained with the indicated antibodies and DAPI. *n* = 3. **(D)** Phosphospecific antibodies were tested on XT or IP with the indicated antibodies or LAP purifications from indicated BAC cells. *n* = 2 experiments. **(E)** Phosphospecific antibodies and antigenic peptides (#, ID number). The phosphosite category as determined by MS and Western blotting (WB) is as follows: i/m, detected in LOG and NOC; m, only in NOC, unphosphorylated in LOG; bi, unphosphorylated in BI; hes, unphosphorylated in Hesp.



Downloaded from [stke.sciencemag.org](http://stke.sciencemag.org) on December 29, 2011

microscopy studies to be located on the backbone of the complex, forming the so-called “arc lamp” domain, and are suggested to control the positioning of the catalytic and regulatory subunits within the APC/C (43–46). We found that two of these TPR subunits, CDC23 and CDC27, had the highest number of phosphorylation events of any of the subunits of the complex (Fig. 4C and table S4), thus suggesting a mechanism by which TPR subunit phosphorylation might regulate APC/C activity during mitosis. Within the cohesin complex, the SMC subunits are thought to play an important structural role holding the sister chromatids together until the onset of anaphase, and the non-SMC subunits have been assigned several regulatory functions (47). The non-SMC subunit WAPAL, for example, is required to remove cohesin from chromosome arms in early mitosis, counteracting the small cohesin subunit cell division cycle associated 5 [CDCA5, also known as sororin (48–50)]. We found that WAPAL was one of the highly phosphorylated cohesin subunits (Fig. 4C and table S4), and it is thus possible that hyperphosphorylation of WAPAL in mitosis plays a role in the regulatory mechanism required to remove chromosome arm-bound cohesin. Identification of PLK1 as the major WAPAL kinase in our study further strengthens this hypothesis, because PLK1 inhibition leads to the accumulation of cohesin on chromosome arms in mitosis (fig. S3G) (24, 51–53). Similar regulatory mechanisms could be at play in the NUP107-160 complex, in which NUP98 and NUP107 are phosphorylated to a much higher proportion than the remaining complex members (Fig. 4C and table S4). The NUP98 subunit is positioned within the complex so that it is exposed to cytosol or nucleoplasm, depending on its localization, and is thus well accessible to protein kinases (54). NUP98 phosphorylation by a number of NIMA-related kinases, but not by PLK1, leads to the disassembly of the nuclear pore complex at mitotic entry (55). We found that the NUP107 subunit (but not NUP98) is a direct PLK1 target (Table 2). It will be important to test how PLK1-dependent phosphorylation of NUP107 influences possible functions of this complex, for example, at the kinetochore in prometaphase (56) where PLK1 is also located (5). Further identification of hyperphosphorylated complex components that possibly serve as kinase regulatory “switchboards” of these complexes opens a way for studying the function of these phosphoregulatory mechanisms during mitotic progression in more detail.

To predict which protein kinases are likely to target the identified phosphosites, we used the Scansite algorithm, which includes PSSMs for 32 kinases, including a set of PSSMs for several mitotic kinases (CDKs, PLK1, AURKA, AURKB, and NEK2) (15). Comparison of the Scansite motifs matched to the sites within our data set with all phosphorylation sites present in the PhosphoSitePlus database (19) revealed not only strong enrichment of the CDK1 motif but also motif enrichment for other proline-directed kinases, such as CDK5 and ERK1. Although the PSSMs used identify minor differences between the CDK1, CDK5, and ERK1 motifs, they all share a strong requirement for proline at the –2 position and absolute requirement for proline at the +1 position (22, 57, 58). Thus, it is possible that the sites that match the motifs for these nonmitotic kinases are CDK1-dependent sites.

To assess the mitosis dependency of phosphorylation sites on mitotic complexes and to identify potential *in vivo* targets of major mitotic kinases that may be important for the regulation of these complexes, we carried out a high sequence coverage analysis of a subset of 12 complexes that comprises major regulators of mitotic chromosome segregation. In contrast to previous proteome-wide studies, this approach allowed a much more complete sequence coverage of the analyzed proteins and yielded many previously unidentified phosphorylation sites on well-studied complexes [compare, for example, the 124 APC/C phosphorylation sites we detected in this study with 59 (11), 71 (9), and 45 sites (25, 42) that had been reported previously]. It will thus be important to expand such

systematic high-coverage analyses to more protein complexes, because these data are likely to yield more informative results on specific subsets of protein complexes and their phosphorylation than previous “proteome-scale” studies.

Small-molecule inhibitors have been used successfully for establishing the involvement of particular protein kinases in biological systems in cell biological experiments (59). With the availability of potent and specific inhibitors of PLK1 and AURKB, we identified several sites that are dependent on PLK1 and AURKB [42 of 400 (11%) and 20 of 400 (5%), respectively]. The percentage of PLK1-dependent sites is lower than that reported in another analysis of the mitotic spindle phosphoproteome, where 18% of all sites were PLK1-dependent [698 of 3984 (13)]. One possibility for this discrepancy is that our nonquantitative MS approach might have missed some phosphorylation sites that were reduced but not completely dephosphorylated after inhibitor treatment. To assess the approximate number of false-negative identifications, we generated a panel of phosphospecific antibodies against sites classified as PLK1-dependent, AURKB-dependent, or independent of either or both of these kinases (Fig. 5 and fig. S5). Two phosphorylation sites on RAD21 (Ser<sup>153</sup> and Ser<sup>175</sup>), which we had classified by MS as PLK1-independent, were PLK1-dependent in this Western blot analysis, suggesting that our approach might have missed several phosphorylation sites that are either only partially dependent on PLK1 or AURKB or that are not fully dephosphorylated after kinase inhibition. A second possibility why in our approach we identified relatively few PLK1- and AURKB-dependent sites is that we acutely inhibited these two kinases in cells that had already entered mitosis. This is in contrast to the study by Santamaria *et al.* (13), where cells entered mitosis in the absence of active PLK1. The sites we identified as lost on complexes purified from inhibitor-treated cells must thus have been actively dephosphorylated by phosphatases. As our understanding of the substrate targeting and activity regulation of phosphatases at present lags behind that of kinases, a new generation of tools will be required to identify the phosphatases that act on PLK1- and AURKB-dependent phosphorylation sites.

Our experiments also revealed that of the eight kinase-dependent sites we tested using phosphospecific antibodies, two sites originally classified as AURKB-dependent (Ser<sup>551</sup> on BUB1B and Thr<sup>1388/89</sup> on NCAPD2) were not AURKB-dependent in Western blot analysis. These sites might have been misclassified because of the low abundance of the corresponding phosphopeptides. In the shotgun MS approach we applied, peptides are selected stochastically for identification; thus, low-abundance peptides have a higher chance of going undetected in complex mixtures of peptides. The targeted MS technique, single-reaction monitoring (SRM), would improve accuracy in the measurement of abundance changes. This is, however, at the cost of the need to select the peptides to be measured before the experiment, thus preventing unbiased sample analysis. Nevertheless, our approach likely identified a large number of true-positive PLK1 and AURKB targets, because 75% (6 of 8) of the phosphospecific antibodies confirmed that the phosphorylation sites identified as kinase sensitive by MS were dependent on PLK1 or AURKB.

Pharmacological kinase inhibition likely results in phosphorylation changes not only on direct targets but also on targets further downstream in the kinase-dependent signaling cascade. Because obtaining evidence for direct kinase-substrate relationships *in vivo* remains virtually impossible, we combined our *in vivo* analysis with Scansite predictions to identify direct targets of PLK1 and AURKB with high confidence. This led to the identification of new candidate direct substrates of PLK1 (RAD21, STAG2, WAPAL, ZWILCH, and NUP107) and AURKB (RAD21), two of which (pSer<sup>1261</sup> on STAG2 and pSer<sup>465</sup> on WAPAL) were phosphorylated on the experimentally identified and computationally predicted sites in *in vitro* kinase assays using recombinant PLK1.

Our study complements the phosphoproteome-wide approaches by an in-depth analysis of many key regulatory complexes and their phosphorylation patterns in mitosis. Because the present study was not designed to generate quantitative data on the stoichiometry of phosphorylation, nor to determine the consequences of phosphorylation (or absence of phosphorylation) at each site, detailed follow-up studies are required to determine the extents and regulatory effects of these phosphorylations on the protein complexes in question. Combination of the MitoCheck localization, interaction, and phosphorylation data [(14, 28), this study], publicly accessible through the MitoCheck (<http://www.mitocheck.org>), PhosphoSitePlus (<http://www.phosphosite.org>), Phospho.ELM (<http://phospho.elm.eu.org>), and PRIDE (<http://www.ebi.ac.uk/pride>) databases, will serve as a resource for further research into the regulation of mitosis. This study shows that the MitoCheck-developed LAP-tagged cell lines allow identification of not only protein localization and protein interactors but also posttranslational modification in a high-throughput fashion. Because many more LAP-tagged proteins are becoming available (60), these cell lines will greatly facilitate systematic analyses of protein complexes regulating many important cellular processes, and our study lays the groundwork for further systematic studies on the phosphorylation of protein complexes.

## MATERIALS AND METHODS

### Cell culture

HeLa cells were cultured on ten 24-cm square cell culture trays, in Dulbecco's modified Eagle's medium (DMEM) supplemented with 10% fetal bovine serum (Gibco/Invitrogen) plus 0.2 mM L-glutamine, penicillin (100 U/ml), and streptomycin (100 µg/ml) (all from Sigma-Aldrich). For transfected cell lines, the medium was supplemented with G418 (500 µg/ml) (Gibco). For Tet-On cell lines, the medium was supplemented with G418 (100 µg/ml) and hygromycin (200 or 400 µg/ml) for maintenance or selection, respectively.

### Cell synchronization and harvesting

To obtain an interphase cell population, we harvested the cells while they were undergoing exponential growth and with a confluence of <90. For those baits (AURKB, CDCA5) whose protein concentrations are low in early interphase but higher in G<sub>2</sub> phase, the cells were harvested after a double-thymidine arrest and release procedure. In one case (PDS5B), the cells were arrested in S phase by inclusion of hydroxyurea in the growth medium for 18 hours. To obtain a cell population arrested in mitosis (prometaphase), we supplemented the culture media of exponentially growing cells with nocodazole at 100 µg/ml, and the cells were incubated for a further 18 hours before harvesting; these cells typically had a mitotic index (as judged by cell morphology) of ≥90%. To obtain cells arrested in mitosis but in which the activity of endogenous PLK1 was inhibited, we incubated nocodazole-treated cells for a further 2 hours with 250 nM BI 4834 (a gift from Boehringer Ingelheim, Vienna, Austria). To obtain cells arrested in mitosis but in which the activity of the endogenous AURKB was inhibited, we incubated nocodazole-arrested cells for a further 2 hours with 100 nM Hesperadin (a gift from Boehringer Ingelheim) plus 10 µM MG132 (Sigma-Aldrich). Cells were harvested by scraping into their medium, washed with ice-cold phosphate-buffered saline (PBS), snap-frozen in liquid nitrogen, and stored at -80°C until required.

### Protein extract preparation

All steps were performed on ice or at 4°C. Frozen cell pellets were thawed and then resuspended in one pellet volume of extract buffer [20 mM tris-HCl (pH 7.5), 150 mM NaCl, 5 mM EDTA, 20 mM β-glycerophosphate, 10 mM NaF, 10% glycerol, 0.1% NP-40, 1 µM okadaic acid (Alexis/Enzo

Life Sciences), 0.2 mM Na<sub>3</sub>VO<sub>4</sub>, 1 mM dithiothreitol, 0.1 mM phenylmethylsulfonyl fluoride, and protease inhibitor mix (leupeptin, pepstatin, and chymostatin, 10 µg/ml each)]. Cells were lysed with a Dounce homogenizer, and the crude extract was clarified by centrifugation at 14,000 rpm in a microfuge for 15 min. The protein concentration of the clarified extracts was estimated by the Bradford method (61) with reagents from Bio-Rad. For a given bait, for each of the different conditions, equal amounts of extract (by mass of protein) were used for the initial affinity purification step.

### Affinity purification of protein complexes

Endogenous proteins were immunopurified with antibodies described in the antibody section. After immunoprecipitation with antibodies cross-linked with dimethyl pimelimidate (62) to Affi-Prep Protein A beads (Bio-Rad), purified complexes were washed extensively in 10× bead volume of IP buffer [extract buffer without phosphatase inhibitors (no β-glycerophosphate, NaF, okadaic acid, or Na<sub>3</sub>VO<sub>4</sub>)] for a total of 1 hour at 4°C. For mass spectrometric analysis, the last three washing steps were performed in IP buffer without detergent.

Purification of protein complexes with LAP-tagged baits was performed as described (28). LAP lysis buffers additionally contained 1 µM okadaic acid and either BI 2536, BI 4834, or Hesperadin combined with MG132 when proteins were purified from inhibitor-treated cells. Purified proteins were eluted from beads with 0.2 M glycine (pH 2.0), and the eluate was neutralized by addition of 1/10 volume of 1.5 M tris-HCl (pH 9.2).

Affinity purification of condensin-I and condensin-II complexes was performed from HeLa cell lines expressing either NCAPH-GFP-FLAG (63) or NCAPH2-GFP-FLAG (64) fusion proteins, respectively. Agarose beads coupled to the M2 antibody recognizing FLAG (65) (Sigma-Aldrich) were washed three times with 150 mM KCl, three times with 0.2 M glycine (pH 2.0), and then three times with IP buffer. Extracts were prepared in LAP lysis buffer containing 1 µM okadaic acid and the relevant kinase inhibitors, as described above. Clarified extract was then mixed with 100 µl of FLAG M2 beads for 1 hour. The beads were pelleted, washed five times with LAP wash buffer (LAP lysis buffer with 0.05% NP-40 instead of 1% Triton X-100) supplemented with 1 µM okadaic acid, and then washed three times with 150 mM KCl. Purified proteins were eluted from the beads with one bed volume of 0.2 M glycine (pH 2.0) and the eluate was neutralized by addition of 1/10 volume of 1.5 M tris-HCl (pH 9.2).

### In-solution digestion of eluted phosphoprotein complexes

Eluted and neutralized protein samples were reduced, acetylated, and subjected to in-solution digestion with trypsin, chymotrypsin, subtilisin, or Glu-C, as described previously (25). About equal amounts of digested peptide mixtures were analyzed by MS.

### MS analysis

All nano-HPLC (high-performance liquid chromatography) separations were performed with an UltiMate 3000 Nano-LC system (Dionex Benelux) equipped with a trap column [PepMap C18, 300-µm inside diameter (ID) × 5-mm length, 3-µm particle size, 100 Å pore size, Dionex] for sample desalting and concentration and an analytical column (PepMap C18, 75-µm ID × 150-mm length, 3-µm particle size, 100 Å pore size, Dionex) for the chromatographic separation. The loading buffer used contained 0.1% trifluoroacetic acid (Pierce/Thermo Scientific). For chromatographic separation, mobile phase A contained 5% acetonitrile (Merck) and 0.1% formic acid (Merck), and mobile phase B contained 80% acetonitrile and 0.08% formic acid. MS analyses were conducted on a hybrid linear ion trap/Fourier transform ion cyclotron resonance (FT-ICR) mass spectrometer (LTQ-FT Ultra, Thermo Fisher Scientific) with a 7-T superconducting

magnet, except for samples derived from NCAPH and NCAPH2 baits, which were analyzed on a 4000 QTRAP mass spectrometer (Applied Biosystems). Mass spectrometers were equipped with a nanoelectrospray ionization (ESI) source (Proxeon Biosystems). Metal-coated nano-ESI needles were used (New Objective).

Samples were loaded onto the trap column at a flow rate of 20  $\mu$ l/min loading buffer and washed for 10 min. Afterward, the sample was eluted from the trap column and separated on the separation column with a gradient from 20 to 50% mobile phase B in 180 min at a flow rate of 300 nl/min.

Peptides eluting from the HPLC were ionized by ESI with a spray voltage set to 1.5 kV. Full-scan measurements [mass/charge ratio ( $m/z$ ) range, 400 to 1800] were conducted in the ICR cell, yielding a survey scan with resolution of 100,000 and a typical mass accuracy of <2 parts per million (ppm). Collision-induced dissociation (CAD) fragmentation and spectrum acquisition were carried out in the linear ion trap with a multistage activation (MSA) method (66). The target values of the automatic gain control were set to 10,000 for CAD in the ion trap and to 500,000 for FT-ICR full-scan spectra. Fragmentation was performed on the five most intense signals of the survey scan with MSA of the neutral loss of phosphoric acid. Singly charged ions were excluded for precursor selection, and precursors of MS<sup>2</sup> spectra acquired in previous scans were excluded for further fragmentation for a period of 3 min, whereas the exclusion mass tolerance was set to 5 ppm.

### Phosphopeptide identification and manual evaluation

MS raw data files were submitted for database searching with the Mascot program (Matrix Science) (17) running on a local computing cluster. For peptide identification, we used a custom sequence database of mouse baits and proteome-wide human proteins as previously described (14). The following parameters were used for the database search: Carboxymethylation (+58.0055 u) of cysteine was set as fixed, and oxidation (+15.9949 u) of methionine and phosphorylation (+79.966331 u) as variable modification; enzymatic cleavage was specified as trypsin, chymotrypsin, or no specificity (for subtilisin digests). Mass tolerances of the parent ion and the fragments were set to 10 ppm and 0.80 dalton, respectively. Unphosphorylated peptides with a Mascot score greater than 20 were kept and used to calculate the sequence coverage of detected proteins after combining all parallel digests (usually trypsin, chymotrypsin, and subtilisin). The result of the Mascot database search for each MS run was exported from the Mascot server as a spreadsheet file in xml format.

After the analysis of phosphorylation sites in the mitotic interaction data set, the relevant Mascot MS data were processed with the Ascore algorithm (18) to provide an additional quality control of the quality of the spectrum-phosphopeptide match.

After Mascot database search of the four-condition data set, for each peptide that Mascot predicted to contain one or more phosphorylated residues, the corresponding MSA spectrum was manually inspected and rated by a single skilled MS data analyst, on a score from 0 to 3, with the criteria described in fig. S4. For each manually rated phosphopeptide, the positions of phosphorylation were indicated within the peptide sequence with the following notation (example given for serine residues): S# represents a phosphorylated residue at a certain position; S% represents one possible position at which a residue may be phosphorylated (the spectrum provides insufficient information to be sure).

### Phosphorylation data set processing

For the four-condition data set, after Mascot database search and manual rating, the total complement of peptide and phosphopeptide data from all experimental conditions was compiled into a custom database. This

allowed the following filters to be applied for each experimental condition: First, where multiple phosphopeptides with identical sequence (and annotation of phosphorylated residues) were present, only the highest-rated ones were kept. Second, where peptides (modified or unmodified) with identical sequence (and annotation of phosphorylated residues, where applicable) were present, only the one with the highest Mascot ions score was kept.

For each bait, the set of sequences of identified peptides (modified or unmodified) was mapped to protein entries in the Ensembl (67) database and used to identify the corresponding Ensembl gene entries, as previously described (14). Peptides mapping to the set of genes defined by our previous analysis (14) as “contaminant” or “background” proteins were identified and removed.

### Phosphosite interpretation

Phosphorylation sites that could not be unambiguously assigned to a single residue were not used further. Unambiguous phosphorylation sites from all four cell cycle conditions were compared: interphase (LOG), mitosis (NOC), mitosis + PLK1 inhibition (BI), and mitosis + AURKB inhibition (Hesp). For each cell cycle state, the phosphorylation site could be either present (P), absent with an unmodified peptide covering the site (N), or absent with no peptide covering the site (nd). We considered only sites that were covered by N, P, or both in all four conditions.

### Antibodies

Phosphospecific antibodies (listed in Fig. 5E) were raised against 8- to 13-mer synthetic peptides (generated in-house with fluorenylmethyloxycarbonyl chemistry) in rabbits and affinity-purified as described (25). The lab internal accession numbers are as follows (the first number corresponds to those shown in Fig. 5E; codes in parentheses are accession codes relevant for antibody requests): 2067 (A768-G), 1706 (A759-M), 1707 (A760-M), 1710 (A761-M), 2063 (A764-M), 1746 (A762-M), 2062 (A763-M), 2263 (A772-G), 2262 (A771-G), 2275 (A775-M), 2068 (A769-G), 2065 (A766-M), 2264 (A773-M), and 2265 (A774-M). Additional antibodies used in immunopurification, Western blotting, and immunofluorescence were as follows: rabbit antibodies recognizing CDC27 (68), PDS5A [antibody number 521 (69)], PDS5B [antibody number 1531: QLKGLDTSKSPQFNRYFC and antibody number 2230: VSTVNVRRRSKRERR (70)], STAG1 [antibody number 444 (69)], STAG2 [antibody number 446 (69)], WAPAL [antibody numbers 986 and 987 (49)], NUP85 (71), NCAPH (72), CDC25C (Cell Signaling Technology), BUB1B (a gift from G. Kohlmaier), INCENP (41), TUBG1 (Sigma-Aldrich), phosphorylated CDC16 (25), RAD21 (Millipore), or PDS5B (Bethyl Laboratories); mouse antibodies recognizing phosphorylated Ser<sup>10</sup> histone H3 (Millipore), CCNB1 (GNS1, Santa Cruz Biotechnology), MYC (Millipore), SMC2 (72), TUBA1B (clone B-5-1-2, Sigma-Aldrich); goat antibody recognizing H3 (Santa Cruz Biotechnology); and a human calcinosis, Raynaud's phenomenon, esophageal dysmotility, sclerodactyly, telangiectasia (CREST) antiserum (Cortex Biochem).

Secondary antibodies used for Western blotting were antibodies recognizing mouse, rabbit, or goat coupled to horseradish peroxidase (HRP); for immunofluorescence, Alexa 488-, Alexa 568-, and Alexa 633-labeled secondary antibodies were used (Molecular Probes/Invitrogen).

### In vitro kinase assays

WAPAL and STAG2 were immunopurified as described above. In vitro phosphorylation was performed as described (25) with 10 mM ATP and recombinant 6 $\times$ His-tagged PLK1. Recombinant human PLK1 was expressed as a 6 $\times$ His-tagged fusion protein with a baculoviral expression system and purified by affinity chromatography with nickel-nitrilotriacetic

acid (NTA)-coupled agarose beads (Qiagen). Where indicated, reactions were supplemented with 1  $\mu$ M BI 2536.

### Histone H1 kinase assays

The activity of a cell extract to catalyze the addition of [ $^{32}$ P]phosphate from [ $\gamma$ - $^{32}$ P]ATP into histone H1 was assayed as described (73). Duplicate measurements were performed twice, and then mean and SD values were calculated. The Bradford method (61) was used to determine the concentration of protein in HeLa cell extracts, and this was used to calculate specific kinase activities (picomoles phosphate incorporated per minute per microgram of extract).

### Immunofluorescence microscopy

Cells were grown on coverslips and fixed with 4% formaldehyde in PBS at room temperature or with methanol at  $-20^{\circ}\text{C}$  for 15 min. RAD21-9 $\times$ MYC cells were centrifuged onto slides (Cytospin, Thermo Scientific), extracted with 0.5% Triton X-100 in PBS for 2 min, and fixed with 4% formaldehyde in PBS (41). After fixation, samples were permeabilized with 0.5% Triton X-100 in PBS for 15 min and thereafter blocked with 10% fetal calf serum in PBS containing 0.01% Triton X-100. Coverslips were incubated for 1 hour each at room temperature with primary and secondary antibodies (at 2  $\mu$ g/ml in 3% bovine serum albumin in PBS containing 0.01% Triton X-100), DNA was counterstained with Hoechst 33342, and samples were mounted with either ProLong Gold (Molecular Probes/Invitrogen) or VECTASHIELD Mounting Medium (H1000, Vector Laboratories) onto slides. Image acquisition was performed as described (74), or (for BI 4834 characterization) images were taken on a Zeiss Axioplan 2 microscope with a 100 $\times$  Plan-Apochromat objective lens (Carl Zeiss) and equipped with a CoolSnap HQ charge-coupled device camera (Photometrics). For signal intensity quantification, images were acquired as raw 12-bit files captured at identical exposure times within each experiment. Images were processed with ImageJ software (<http://rsb.info.nih.gov/ij/>) (75). Images shown in the same panel have been scaled identically.

For quantification of TUBG1 intensities, a circular region with a fixed diameter was measured on the centrosome and a same-sized region was also measured in the cytoplasm. After the background outside the cells was subtracted, the ratio of these values was calculated and the average and SD of these measurements were plotted. For each measurement, at least 40 centrosomes in 20 cells were quantified. Mitotic phenotypes were classified on the basis of the staining pattern produced by 4',6-diamidino-2-phenylindole (DAPI) and TUBA1B antibodies; for each measurement, 100 cells were counted.

### Scansite and statistical analyses

Scansite predicts potential target sites for a protein kinase by scanning through a set of protein sequences, evaluating for each Ser, Thr, or Tyr residue the match between its surrounding sequence and the preferred amino acids in each position relative to the target site, as represented by a PSSM (20, 21).

We established an automated computing workflow enabling the Scansite algorithm, running on a local server, to scan a large set of input protein sequences, using multiple PSSMs in succession. This approach was used to predict which kinases may target particular Ser, Thr, or Tyr residues among the set of protein sequences in which phosphosites were identified by MS. Each match between a PSSM and a Ser, Thr, or Tyr residue and its surrounding sequence is given a score (the "Scansite score") and is assigned a percentile. The percentile is based on the position of the Scansite score in the empiric score distribution derived from a reference data set. Because the phosphosites in our data set are recorded as positions relative to protein entries from the Ensembl database (<http://www.ensembl.org>) (67), a complete set of Ensembl human and mouse protein sequences was used as the reference data set. We considered Scansite hits within the 5,  $\leq 1.5$ , and  $\leq 0.2\%$  as "low," "medium," and "high" stringency, respectively. We only included hits of high or medium stringency in the analytical outputs.

Statistical analyses were performed to determine whether the number of Scansite hits matching MS-derived phosphosites was significantly greater than that which we would expect on the basis of the known distribution of phosphosites in the human proteome. The number of matches of Scansite hits to phosphosites recorded in the PhosphoSitePlus database (<http://www.phosphosite.org>) (19) was determined. For each kinase motif, a Bonferroni-corrected Fisher's exact test (76) was used to calculate the probability ( $P$  value) that our set of MS-identified phosphosites would have been found at the same frequency by chance alone. To make the reporting of  $P$  values (which vary across an exponential range) more manageable, they were expressed as a probability score, equal to  $-\log_{10}(P)$ . Kinase motifs with a probability score of 2 or greater (where the corrected probability of a random match was 1 in 100 or lower) were considered significant.

Statistical analyses were performed to determine whether the number of Scansite hits matching MS-derived phosphosites was significantly greater than that which we would expect on the basis of the known distribution of phosphosites in the human proteome. The number of matches of Scansite hits to phosphosites recorded in the PhosphoSitePlus database (<http://www.phosphosite.org>) (19) was determined. For each kinase motif, a Bonferroni-corrected Fisher's exact test (76) was used to calculate the probability ( $P$  value) that our set of MS-identified phosphosites would have been found at the same frequency by chance alone. To make the reporting of  $P$  values (which vary across an exponential range) more manageable, they were expressed as a probability score, equal to  $-\log_{10}(P)$ . Kinase motifs with a probability score of 2 or greater (where the corrected probability of a random match was 1 in 100 or lower) were considered significant.

### SUPPLEMENTARY MATERIALS

[www.sciencesignaling.org/cgi/content/full/4/198/rs12/DC1](http://www.sciencesignaling.org/cgi/content/full/4/198/rs12/DC1)

Fig. S1. Visualization of phosphosites within the human mitotic interaction network with Cytoscape.

Fig. S2. Statistical analysis of the frequency of occurrence of kinase motifs matching phosphosites in the mitotic interaction data set.

Fig. S3. BI 4834 is structurally and functionally related to BI 2536.

Fig. S4. Manual evaluation of phosphopeptide multistage activation (MSA) spectra.

Fig. S5. Further analysis with phosphospecific antibodies.

Table S1. List of all detected phosphorylation sites in the interaction data set, including Scansite matches and Ascores.

Table S2. List of sequence coverages for the proteins analyzed in the interaction data set, including phosphorylation site densities in percent.

Table S3. List of all detected phosphorylation sites in the four-condition data set, including Scansite matches.

Table S4. List of sequence coverages for the proteins analyzed in the four-condition set, including phosphorylation site densities in percent.

Table S5. Access to experimental and RAW file data.

Cytoscape file S1. Interaction data set, including information on cluster membership, number of phosphorylation sites, phosphorylation site density in percent, and protein sequence coverage.

### REFERENCES AND NOTES

1. B. Alberts, The cell as a collection of protein machines: Preparing the next generation of molecular biologists. *Cell* **92**, 291–294 (1998).
2. A. Chari, U. Fischer, Cellular strategies for the assembly of molecular machines. *Trends Biochem. Sci.* **35**, 676–683 (2010).
3. T. J. Mitchison, Microtubule dynamics and kinetochore function in mitosis. *Annu. Rev. Cell Biol.* **4**, 527–549 (1988).
4. Here, proteins are referred to by their official gene symbols: for human genes according to the Human Genome Organization (HUGO) nomenclature (<http://www.genenames.org>); for mouse genes, according to the Mouse Genome Informatics (MGI) nomenclature (<http://www.informatics.jax.org>).
5. E. A. Nigg, Mitotic kinases as regulators of cell division and its checkpoints. *Nat. Rev. Mol. Cell Biol.* **2**, 21–32 (2001).
6. J. M. Peters, The anaphase promoting complex/cyclosome: A machine designed to destroy. *Nat. Rev. Mol. Cell Biol.* **7**, 644–656 (2006).
7. A. Musacchio, E. D. Salmon, The spindle-assembly checkpoint in space and time. *Nat. Rev. Mol. Cell Biol.* **8**, 379–393 (2007).
8. M. Nousiainen, H. H. Silljé, G. Sauer, E. A. Nigg, R. Körner, Phosphoproteome analysis of the human mitotic spindle. *Proc. Natl. Acad. Sci. U.S.A.* **103**, 5391–5396 (2006).
9. J. A. Steen, H. Steen, A. Georgi, K. Parker, M. Springer, M. Kirchner, F. Hamprecht, M. W. Kirschner, Different phosphorylation states of the anaphase promoting complex in response to antimetabolic drugs: A quantitative proteomic analysis. *Proc. Natl. Acad. Sci. U.S.A.* **105**, 6069–6074 (2008).

10. R. Malik, R. Lenobel, A. Santamaria, A. Ries, E. A. Nigg, R. Körner, Quantitative analysis of the human spindle phosphoproteome at distinct mitotic stages. *J. Proteome Res.* **8**, 4553–4563 (2009).
11. J. V. Olsen, M. Vermeulen, A. Santamaria, C. Kumar, M. L. Miller, L. J. Jensen, F. Gnäd, J. Cox, T. S. Jensen, E. A. Nigg, S. Brunak, M. Mann, Quantitative phosphoproteomics reveals widespread full phosphorylation site occupancy during mitosis. *Sci. Signal.* **3**, ra3 (2010).
12. N. Dephoure, C. Zhou, J. Villén, S. A. Beausoleil, C. E. Bakalarski, S. J. Elledge, S. P. Gygi, A quantitative atlas of mitotic phosphorylation. *Proc. Natl. Acad. Sci. U.S.A.* **105**, 10762–10767 (2008).
13. A. Santamaria, B. Wang, S. Elowe, R. Malik, F. Zhang, M. Bauer, A. Schmidt, H. H. Silljé, R. Körner, E. A. Nigg, The Plk1-dependent phosphoproteome of the early mitotic spindle. *Mol. Cell. Proteomics* **10**, M110.004457 (2011).
14. J. R. A. Hutchins, Y. Toyoda, B. Hegemann, I. Poser, J. K. Hériché, M. M. Sykora, M. Augsburg, O. Hudecz, B. A. Buschhorn, J. Bulkescher, C. Conrad, D. Comartin, A. Schleiffer, M. Sarov, A. Pozniakovskiy, M. M. Slabicki, S. Schloissnig, I. Steinmacher, M. Leuschner, A. Ssykor, S. Lawo, L. Pelletier, H. Stark, K. Nasmyth, J. Ellenberg, R. Durbin, F. Buchholz, K. Mechtler, A. A. Hyman, J. M. Peters, Systematic analysis of human protein complex identifiers chromosome segregation proteins. *Science* **328**, 593–599 (2010).
15. J. Alexander, D. Lim, B. A. Joughin, B. Hegemann, J. R. Hutchins, T. Ehrenberger, F. Ivins, F. Sessa, O. Hudecz, E. A. Nigg, A. M. Fry, A. Musacchio, P. T. Stukenberg, K. Mechtler, J. M. Peters, S. J. Smerdon, M. B. Yaffe, Spatial exclusivity combined with positive and negative selection of phosphorylation motifs is the basis for context-dependent mitotic signaling. *Sci. Signal.* **4**, ra42 (2011).
16. S. Hauf, R. W. Cole, S. LaTerra, C. Zimmer, G. Schnapp, R. Walter, A. Heckel, J. van Meel, C. L. Rieder, J. M. Peters, The small molecule Hesperadin reveals a role for Aurora B in correcting kinetochore–microtubule attachment and in maintaining the spindle assembly checkpoint. *J. Cell Biol.* **161**, 281–294 (2003).
17. D. N. Perkins, D. J. Pappin, D. M. Creasy, J. S. Cottrell, Probability-based protein identification by searching sequence databases using mass spectrometry data. *Electrophoresis* **20**, 3551–3567 (1999).
18. S. A. Beausoleil, J. Villén, S. A. Gerber, J. Rush, S. P. Gygi, A probability-based approach for high-throughput protein phosphorylation analysis and site localization. *Nat. Biotechnol.* **24**, 1285–1292 (2006).
19. P. V. Hornbeck, I. Chabra, J. M. Kornhauser, E. Skrzypek, B. Zhang, PhosphoSite: A bioinformatics resource dedicated to physiological protein phosphorylation. *Proteomics* **4**, 1551–1561 (2004).
20. J. C. Obenauer, L. C. Cantley, M. B. Yaffe, Scansite 2.0: Proteome-wide prediction of cell signaling interactions using short sequence motifs. *Nucleic Acids Res.* **31**, 3635–3641 (2003).
21. M. B. Yaffe, G. G. Lepar, J. Lai, T. Obata, S. Volinia, L. C. Cantley, A motif-based profile scanning approach for genome-wide prediction of signaling pathways. *Nat. Biotechnol.* **19**, 348–353 (2001).
22. G. Panchamoorthy, T. Fukazawa, L. Stolz, G. Payne, K. Reedquist, S. Shoelson, Z. Songyang, L. Cantley, C. Walsh, H. Band, Physical and functional interactions between SH2 and SH3 domains of the Src family protein tyrosine kinase p59fyn. *Mol. Cell Biol.* **14**, 6372–6385 (1994).
23. J. Gautier, C. Norbury, M. Lohka, P. Nurse, J. Maller, Purified maturation-promoting factor contains the product of a *Xenopus* homolog of the fission yeast cell cycle control gene *cdc2<sup>+</sup>*. *Cell* **54**, 433–439 (1988).
24. P. Lénárt, M. Petronczki, M. Steegmaier, B. Di Fiore, J. J. Lipp, M. Hoffmann, W. J. Rettig, N. Kraut, J. M. Peters, The small-molecule inhibitor BI 2536 reveals novel insights into mitotic roles of Polo-like kinase 1. *Curr. Biol.* **17**, 304–315 (2007).
25. C. Kraft, F. Herzog, C. Gieffers, K. Mechtler, A. Hagting, J. Pines, J. M. Peters, Mitotic regulation of the human anaphase-promoting complex by phosphorylation. *EMBO J.* **22**, 6598–6609 (2003).
26. S. Elowe, S. Hümmer, A. Uldschmid, X. Li, E. A. Nigg, Tension-sensitive Plk1 phosphorylation on BubR1 regulates the stability of kinetochore microtubule interactions. *Genes Dev.* **21**, 2205–2219 (2007).
27. I. M. Cheeseman, A. Desai, A combined approach for the localization and tandem affinity purification of protein complexes from metazoans. *Sci. STKE* **2005**, pl1 (2005).
28. I. Poser, M. Sarov, J. R. A. Hutchins, J. K. Hériché, Y. Toyoda, A. Pozniakovskiy, D. Weigl, A. Nitzsche, B. Hegemann, A. W. Bird, L. Pelletier, R. Kittler, S. Hua, R. Naumann, M. Augsburg, M. M. Sykora, H. Hofemeister, Y. Zhang, K. Nasmyth, K. P. White, S. Dietzel, K. Mechtler, R. Durbin, A. F. Stewart, J. M. Peters, F. Buchholz, A. A. Hyman, BAC TransgeneOmics: A high-throughput method for exploration of protein function in mammals. *Nat. Methods* **5**, 409–415 (2008).
29. B. Neumann, T. Walter, J. K. Hériché, J. Bulkescher, H. Erfle, C. Conrad, P. Rogers, I. Poser, M. Held, U. Liebel, C. Cetin, F. Sieckmann, G. Pau, R. Kabbe, A. Wünsche, V. Satagopam, M. H. Schmitz, C. Chapuis, D. W. Gerlich, R. Schneider, R. Eils, W. Huber, J. M. Peters, A. A. Hyman, R. Durbin, R. Pepperkok, J. Ellenberg, Phenotypic profiling of the human genome by time-lapse microscopy reveals cell division genes. *Nature* **464**, 721–727 (2010).
30. W. Qi, Z. Tang, H. Yu, Phosphorylation- and polo-box-dependent binding of Plk1 to Bub1 is required for the kinetochore localization of Plk1. *Mol. Biol. Cell* **17**, 3705–3716 (2006).
31. Y. H. Chi, K. Haller, M. D. Ward, O. J. Semmes, Y. Li, K. T. Jeang, Requirements for protein phosphorylation and the kinase activity of polo-like kinase 1 (Plk1) for the kinetochore function of mitotic arrest deficiency protein 1 (Mad1). *J. Biol. Chem.* **283**, 35834–35844 (2008).
32. T. Hirota, J. J. Lipp, B. H. Toh, J. M. Peters, Histone H3 serine 10 phosphorylation by Aurora B causes HP1 dissociation from heterochromatin. *Nature* **438**, 1176–1180 (2005).
33. W. Fischle, B. S. Tseng, H. L. Dormann, B. M. Ueberheide, B. A. Garcia, J. Shabanowitz, D. F. Hunt, H. Funabiki, C. D. Allis, Regulation of HP1-chromatin binding by histone H3 methylation and phosphorylation. *Nature* **438**, 1116–1122 (2005).
34. R. Honda, R. Körner, E. A. Nigg, Exploring the functional interactions between Aurora B, INCENP, and survivin in mitosis. *Mol. Biol. Cell* **14**, 3325–3341 (2003).
35. H. Dinkel, C. Chica, A. Via, C. M. Gould, L. J. Jensen, T. J. Gibson, F. Diella, PhosphoELM: A database of phosphorylation sites—Update 2011. *Nucleic Acids Res.* **39**, D261–D267 (2011).
36. J. A. Vizcaino, R. Côté, F. Reisinger, J. M. Foster, M. Mueller, J. Rameseder, H. Hermjakob, L. Martens, A guide to the Proteomics Identifications Database proteomics data repository. *Proteomics* **9**, 4276–4283 (2009).
37. J. Maller, M. Wu, J. C. Gerhart, Changes in protein phosphorylation accompanying maturation of *Xenopus laevis* oocytes. *Dev. Biol.* **58**, 295–312 (1977).
38. E. Karsenti, R. Bravo, M. Kirschner, Phosphorylation changes associated with the early cell cycle in *Xenopus* eggs. *Dev. Biol.* **119**, 442–453 (1987).
39. R. Malik, E. A. Nigg, R. Körner, Comparative conservation analysis of the human mitotic phosphoproteome. *Bioinformatics* **24**, 1426–1432 (2008).
40. B. Bodenmiller, S. Wanka, C. Kraft, J. Urban, D. Campbell, P. G. Pedrioli, B. Gerrits, P. Picotti, H. Lam, O. Vitek, M. Y. Brusniak, B. Roschitzki, C. Zhang, K. M. Shokat, R. Schlapbach, A. Colman-Lerner, G. P. Nolan, A. I. Nesvizhskii, M. Peter, R. Loewith, C. von Mering, R. Aebersold, Phosphoproteomic analysis reveals interconnected system-wide responses to perturbations of kinases and phosphatases in yeast. *Sci. Signal.* **3**, rs4 (2010).
41. S. Hauf, E. Roitinger, B. Koch, C. M. Dittrich, K. Mechtler, J. M. Peters, Dissociation of cohesin from chromosome arms and loss of arm cohesion during early mitosis depends on phosphorylation of SA2. *PLoS Biol.* **3**, e69 (2005).
42. F. Herzog, K. Mechtler, J. M. Peters, Identification of cell cycle-dependent phosphorylation sites on the anaphase-promoting complex/cyclosome by mass spectrometry. *Methods Enzymol.* **398**, 231–245 (2005).
43. P. Dube, F. Herzog, C. Gieffers, B. Sander, D. Riedel, S. A. Müller, A. Engel, J. M. Peters, H. Stark, Localization of the coactivator Cdh1 and the cullin subunit Apc2 in a cryo-electron microscopy model of vertebrate APC/C. *Mol. Cell* **20**, 867–879 (2005).
44. F. Herzog, I. Primorac, P. Dube, P. Lénárt, B. Sander, K. Mechtler, H. Stark, J. M. Peters, Structure of the anaphase-promoting complex/cyclosome interacting with a mitotic checkpoint complex. *Science* **323**, 1477–1481 (2009).
45. B. A. Buschhorn, G. Petzold, M. Galova, P. Dube, C. Kraft, F. Herzog, H. Stark, J. M. Peters, Substrate binding on the APC/C occurs between the coactivator Cdh1 and the processivity factor Doc1. *Nat. Struct. Mol. Biol.* **18**, 6–13 (2011).
46. P. C. da Fonseca, E. H. Kong, Z. Zhang, A. Schreiber, M. A. Williams, E. P. Morris, D. Barford, Structures of APC/C<sup>Cdh1</sup> with substrates identify Cdh1 and Apc10 as the D-box co-receptor. *Nature* **470**, 274–278 (2011).
47. J. M. Peters, A. Tedeschi, J. Schmitz, The cohesin complex and its roles in chromosome biology. *Genes Dev.* **22**, 3089–3114 (2008).
48. R. Gandhi, P. J. Gillespie, T. Hirano, Human Wapl is a cohesin-binding protein that promotes sister-chromatid resolution in mitotic prophase. *Curr. Biol.* **16**, 2406–2417 (2006).
49. S. Kueng, B. Hegemann, B. H. Peters, J. J. Lipp, A. Schleiffer, K. Mechtler, J. M. Peters, Wapl controls the dynamic association of cohesin with chromatin. *Cell* **127**, 955–967 (2006).
50. T. Nishiyama, R. Ladurner, J. Schmitz, E. Kreidl, A. Schleiffer, V. Bhaskara, M. Bando, K. Shirahige, A. A. Hyman, K. Mechtler, J. M. Peters, Sororin mediates sister chromatid cohesion by antagonizing Wapl. *Cell* **143**, 737–749 (2010).
51. A. Losada, M. Hirano, T. Hirano, Cohesin release is required for sister chromatid resolution, but not for condensin-mediated compaction, at the onset of mitosis. *Genes Dev.* **16**, 3004–3016 (2002).
52. I. Sumara, E. Vorlaufer, P. T. Stukenberg, O. Kelm, N. Redemann, E. A. Nigg, J. M. Peters, The dissociation of cohesin from chromosomes in prophase is regulated by Polo-like kinase. *Mol. Cell* **9**, 515–525 (2002).
53. J. F. Giménez-Abián, I. Sumara, T. Hirota, S. Hauf, D. Gerlich, C. de la Torre, J. Ellenberg, J. M. Peters, Regulation of sister chromatid cohesion between chromosome arms. *Curr. Biol.* **14**, 1187–1193 (2004).
54. E. R. Griffis, S. Xu, M. A. Powers, Nup98 localizes to both nuclear and cytoplasmic sides of the nuclear pore and binds to two distinct nucleoporin subcomplexes. *Mol. Biol. Cell* **14**, 600–610 (2003).

55. E. Laurrell, K. Beck, K. Krupina, G. Theerthagiri, B. Bodenmiller, P. Horvath, R. Aebersold, W. Antonin, U. Kutay, Phosphorylation of Nup98 by multiple kinases is crucial for NPC disassembly during mitotic entry. *Cell* **144**, 539–550 (2011).
56. S. Güttinger, E. Laurrell, U. Kutay, Orchestrating nuclear envelope disassembly and reassembly during mitosis. *Nat. Rev. Mol. Cell Biol.* **10**, 178–191 (2009).
57. Z. Songyang, K. P. Lu, Y. T. Kwon, L. H. Tsai, O. Filhol, C. Cochet, D. A. Brickey, T. R. Soderling, C. Bartleson, D. J. Graves, A. J. DeMaggio, M. F. Hoekstra, J. Blenis, T. Hunter, L. C. Cantley, A structural basis for substrate specificities of protein Ser/Thr kinases: Primary sequence preference of casein kinases I and II, NIMA, phosphorylase kinase, calmodulin-dependent kinase II, CDK5, and Erk1. *Mol. Cell Biol.* **16**, 6486–6493 (1996).
58. I. A. Manke, A. Nguyen, D. Lim, M. Q. Stewart, A. E. Elia, M. B. Yaffe, MAPKAP kinase-2 is a cell cycle checkpoint kinase that regulates the G<sub>2</sub>/M transition and S phase progression in response to UV irradiation. *Mol. Cell* **17**, 37–48 (2005).
59. P. Cohen, Targeting protein kinases for the development of anti-inflammatory drugs. *Curr. Opin. Cell Biol.* **21**, 317–324 (2009).
60. N. C. Hubner, A. W. Bird, J. Cox, B. Spletstoeser, P. Bandilla, I. Poser, A. Hyman, M. Mann, Quantitative proteomics combined with BAC TransgeneOmics reveals in vivo protein interactions. *J. Cell Biol.* **189**, 739–754 (2010).
61. M. M. Bradford, A rapid and sensitive method for the quantitation of microgram quantities of protein utilizing the principle of protein-dye binding. *Anal. Biochem.* **72**, 248–254 (1976).
62. E. Harlow, D. Lane, *Using Antibodies: A Laboratory Manual* (Cold Spring Harbor Laboratory Press, Cold Spring Harbor, NY, ed. 1, 1999).
63. T. Hirota, D. Gerlich, B. Koch, J. Ellenberg, J. M. Peters, Distinct functions of condensin I and II in mitotic chromosome assembly. *J. Cell Sci.* **117**, 6435–6445 (2004).
64. D. Gerlich, T. Hirota, B. Koch, J. M. Peters, J. Ellenberg, Condensin I stabilizes chromosomes mechanically through a dynamic interaction in live cells. *Curr. Biol.* **16**, 333–344 (2006).
65. B. L. Brizzard, R. G. Chubet, D. L. Vizard, Immunoaffinity purification of FLAG epitope-tagged bacterial alkaline phosphatase using a novel monoclonal antibody and peptide elution. *Biotechniques* **16**, 730–735 (1994).
66. M. J. Schroeder, J. Shabanowitz, J. C. Schwartz, D. F. Hunt, J. J. Coon, A neutral loss activation method for improved phosphopeptide sequence analysis by quadrupole ion trap mass spectrometry. *Anal. Chem.* **76**, 3590–3598 (2004).
67. P. Flicek, M. R. Amodè, D. Barrell, K. Beal, S. Brent, Y. Chen, P. Clapham, G. Coates, S. Fairley, S. Fitzgerald, L. Gordon, M. Hendrix, T. Hourlier, N. Johnson, A. Kahari, D. Keefe, S. Keenan, R. Kinsella, F. Kokocinski, E. Kulesha, P. Larsson, I. Longden, W. McLaren, B. Overduin, B. Pritchard, H. S. Riat, D. Rios, G. R. Ritchie, M. Ruffier, M. Schuster, D. Sobral, G. Spudich, Y. A. Tang, S. Trevanion, J. Vandrovцова, A. J. Vilella, S. White, S. P. Wilder, A. Zadissa, J. Zamora, B. L. Aken, E. Birney, F. Cunningham, I. Dunham, R. Durbin, X. M. Fernández-Suarez, J. Herrero, T. J. Hubbard, A. Parker, G. Proctor, J. Vogel, S. M. Searle, Ensembl 2011. *Nucleic Acids Res.* **39**, D800–D806 (2011).
68. C. Gieffers, B. H. Peters, E. R. Kramer, C. G. Dotti, J. M. Peters, Expression of the CDH1-associated form of the anaphase-promoting complex in postmitotic neurons. *Proc. Natl. Acad. Sci. U.S.A.* **96**, 11317–11322 (1999).
69. I. Sumara, E. Vorlaufer, C. Gieffers, B. H. Peters, J. M. Peters, Characterization of vertebrate cohesin complexes and their regulation in prophase. *J. Cell Biol.* **151**, 749–762 (2000).
70. A. Losada, T. Yokochi, T. Hirano, Functional contribution of Pds5 to cohesin-mediated cohesion in human cells and *Xenopus* egg extracts. *J. Cell Sci.* **118**, 2133–2141 (2005).
71. I. Loïdice, A. Alves, G. Rabut, M. Van Overbeek, J. Ellenberg, J. B. Sibarita, V. Doye, The entire Nup107-160 complex, including three new members, is targeted as one entity to kinetochores in mitosis. *Mol. Biol. Cell* **15**, 3333–3344 (2004).
72. F. M. Yeong, H. Hombauer, K. S. Wendt, T. Hirota, I. Mudrak, K. Mechtler, T. Loregger, A. Marchler-Bauer, K. Tanaka, J. M. Peters, E. Ogris, Identification of a subunit of a novel Kleisin- $\beta$ /SMC complex as a potential substrate of protein phosphatase 2A. *Curr. Biol.* **13**, 2058–2064 (2003).
73. P. R. Clarke, in *Cell Cycle: Materials and Methods*, M. Pagano, Ed. (Springer, Heidelberg, 1995), pp. 103–116.
74. I. C. Waizenegger, S. Hauf, A. Meinke, J. M. Peters, Two distinct pathways remove mammalian cohesin from chromosome arms in prophase and from centromeres in anaphase. *Cell* **103**, 399–410 (2000).
75. T. J. Collins, ImageJ for microscopy. *Biotechniques* **43** (suppl.), S25–S30 (2007).
76. R. A. Fisher, *Statistical Methods for Research Workers* (Oliver and Boyd, Edinburgh, UK, ed. 13, 1958).
77. Student, The probable error of a mean. *Biometrika* **6**, 1–25 (1908).
78. **Acknowledgments:** We thank E. Kreidl, G. G. Leparç, M. Madalinski, G. Mitulović, M. Schutzbier, I. Steinmacher, Y. Sun, and S. Zettl [Research Institute of Molecular Pathology–Institute of Molecular Biotechnology (IMP-IMBA), Vienna], and M. Augsburg, F. Buchholz, D. Richter, and A. Szykor [Max Planck Institute of Molecular Cell Biology and Genetics (MPI-CBG), Dresden] for valuable advice and assistance; V. Doye (Institut Curie, Paris) for the gift of the anti-NUP85 antibody; S. Beausoleil (Harvard University) for Ascore analysis of Mascot results; M. Peter (Eidgenössische Technische Hochschule, Zürich) for providing lab space and reagents during revision experiments; and R. Durbin, J. Ellenberg, and K. Nasmyth for helpful discussions. **Funding:** This work was funded by the European Commission through the Sixth Framework Programme Integrated Project “MitoCheck” (LSHG-CT-2004-503464). Work in the laboratories of J.-M.P. and K.M. received support from Boehringer Ingelheim, the Austrian Science Fund Special Research Programme F34 “Chromosome Dynamics,” and the Austrian Research Promotion Agency FFG. Work in the laboratory of M.B.Y. was funded, in part, by NIH grants GM-60594, GM-68762, ES-015339, and CA-112967. **Author contributions:** B.H., J.R.A.H., M.M.S., P.L., and J.-M.P. designed and/or performed wet bench experiments and interpreted results. O.H., M.N., M.M., and J.-K.H. performed data and bioinformatics analyses. J.R., S.L., and M.B.Y. designed and performed computational experiments. I.P., N.K., and A.A.H. generated essential reagents. A.A.H., M.B.Y., K.M., and J.-M.P. supervised the project. B.H., J.R.A.H., and J.-M.P. wrote the manuscript. **Competing interests:** It is the policy of IMP, IMBA, CBG, and Massachusetts Institute of Technology to fulfill all reasonable requests for materials, but in certain cases a material transfer agreement may be required. N.K. is an employee of Boehringer Ingelheim RCV GmbH & Co KG, which supplied the compounds Hesperadin and BI 4834 used in this study, holds two patents on some of the phosphorylation sites published here (EP1884522 for WAPAL, EP1884523 for STAG2), and in part funded this research. **Data availability:** MS results and peptide spectra are available at the PRIDE database (<http://www.ebi.ac.uk/pride>): accession code 12224 (“interaction” data set), and accession codes 11797 to 12223 (“four-condition” data set). MS raw data files are available for download from an IMP-hosted server; see table S5 for full information.

Submitted 8 March 2011

Accepted 20 October 2011

Final Publication 8 November 2011

10.1126/scisignal.2001993

**Citation:** B. Hegemann, J. R. A. Hutchins, O. Hudec, M. Novatchkova, J. Rameseder, M. M. Sykora, S. Liu, M. Mazanek, P. Lénárt, J.-K. Hériché, I. Poser, N. Kraut, A. A. Hyman, M. B. Yaffe, K. Mechtler, J.-M. Peters, Systematic phosphorylation analysis of human mitotic protein complexes. *Sci. Signal.* **4**, rs12 (2011).